Chemical Engineering Research and Design 200 (2023) 550–565

Contents lists available at ScienceDirect

Chemical Engineering Research and Design

journal homepage: www.elsevier.com/locate/cherd

Life cycle environmental impact assessment of slaughterhouse wastewater treatment

Chuan Jiet Teo [a,b,*], Efthalia Karkou [c,**], Ozana Vlad [d], Antonia Vyrkou [d], Nikolaos Savvakis [c], George Arampatzis [c], Athanasios Angelis-Dimakis [d]

[a] KWR Water Research Institute, Water Treatment & Resource Recovery, Groningenhaven 7, 3430 BB Nieuwegein, the Netherlands
[b] Institute of Environmental Engineering, RWTH Aachen University, Mies-van-der-Rohe-Strasse 1, D-52074 Aachen, Germany
[c] School of Production Engineering and Management, Technical University of Crete, Chania, Greece
[d] Department of Chemical Sciences, School of Applied Sciences, University of Huddersfield, Queensgate, HD1 3DH Huddersfield, UK

ARTICLE INFO

Keywords:
Wastewater treatment
Process modelling
Life Cycle Assessment
Slaughterhouse

ABSTRACT

Slaughterhouses are significant industrial water users, ranking second highest in the livestock processing sector, and a potential pollution source for water bodies due to effluent discharge. This paper uses the wastewater composition of an actual slaughterhouse and models three alternative scenarios for the wastewater management; no treatment and discharge, primary treatment and discharge, and tertiary treatment followed by partial water reuse. All three scenarios are assessed in terms of their environmental performance following a Life Cycle Assessment, by using the Environmental Footprint 3.0 method. The results revealed that the best scenario for the slaughterhouse wastewater treatment is the third scenario with an overall footprint of 0.255 milliEcopoints (mPt), compared to 2.45 mPt and 1.31 mPt of the first and the second scenario, respectively.

1. Introduction

Being one of the most dynamic parts of the agricultural sector, the rapid changes in the livestock sector are highly driven by population growth, rising affluence and urbanisation (Managing Water Report under Uncertainty and Risk, 2012). Whilst the increase in demand for livestock production and processing has constituted economic growth, it is also inherently being matched to an increase in its impacts on the environment (Valta et al., 2015). In the value chain of livestock processing, a slaughterhouse is the second largest user of water, and a potentially significant point source of pollution to local ecosystems. Furthermore, some of the most significant environmental issues associated with slaughterhouse operation are water depletion, wastewater pollution, and energy consumption (Genné and Derden, 2008). Regardless of the discussion on the trade-off between the benefits and drawbacks of the slaughterhouse operation, the increasing demand for livestock is nowadays inevitable, indicating that improving resource efficiency is now an urgent priority, especially towards more sustainable water use practices and wastewater management strategies (Lundqvist et al., 2008). A decentralised wastewater treatment, in association with local organisations and governance, is increasingly recognised as one of the options to contribute towards an improved wastewater treatment and the recovery and reuse of the treated wastewater (Libralato et al., 2012). Libralato et al. (2012) have comprehensively compared a centralised and a decentralised wastewater treatment system. The study shows that the latter offers several benefits, including the prevention of decreased surface water quality, a higher potential to support wastewater recovery, maximised reuse and improved environmental sustainability. The environmental benefits of a decentralised wastewater treatment as described by (Libralato et al., 2012) coincide with several other studies (Tchobanoglous, 2003; Brown et al., 2010; Tchobanoglous et al., 2004; Ho and Martin, 2006).

A typical wastewater stream produced by the slaughterhouse operation is characterised by a high concentration of pollutants, such as total suspended solids (TSS), oil and grease. It is rich in total carbon (TC), total nitrogen (TN), total phosphorus (TP) and is characterised by large amounts of chemical oxygen demand (COD) and biological oxygen demand (BOD). A common practice for the management of wastewater derived from slaughterhouses is the pre-treatment stage and then discharge to the municipal wastewater treatment plant, aspiring to be

* Corresponding authors at: KWR Water Research Institute, Water Treatment & Resource Recovery, Groningenhaven 7, 3430 BB Nieuwegein, the Netherlands.
** Corresponding author.
E-mail addresses: chuan.jiet.teo@rwth-aachen.de, chuan.jiet.teo@kwrwater.nl (C.J. Teo), ekarkou@tuc.gr (E. Karkou).

https://doi.org/10.1016/j.cherd.2023.11.016
Received 12 May 2023; Received in revised form 8 November 2023; Accepted 11 November 2023
Available online 17 November 2023

released safely to the environment (Bustillo-Lecompte and Mehrvar, 2017). Biological treatment is commonly used to treat slaughterhouse wastewater, due to its relatively low cost and the effective removal of the aforementioned pollutants. Different biological treatment technologies have been studied on slaughterhouse wastewater, including activated sludge process, membrane bioreactor, upflow anaerobic sludge blanket reactor, granular bed reactor, and anaerobic filters demonstrating the effectiveness (i.e. more than 80% COD removal) of the biological treatment on slaughterhouse wastewater with concentrated pollutant load (Valta et al., 2015; Bustillo-Lecompte and Mehrvar, 2017; Gerbens-Leenes et al., 2013; Davarnejad and Nasiri, 2017; Jensen et al., 2015; Del Nery et al., 2007; Liu et al., 2015; Aziz et al., 2019). However, the sensitivity in higher temperatures, the inability to remove nutrients, such as nitrates and phosphates, the production of low to moderate quality products, and the requirement for longer start-up periods and high hydraulic retention time have led to the exclusion of anaerobic processes (Aziz et al., 2019; Gutu et al., 2021; Musa and Idrus, 2021). In recent studies, the possibility of complimenting biological treatment with advanced oxidation processes has been studied for improved removal of organics and for disinfection in the context of water reuse (Ahmed et al., 2022; Deng and Zhao, 2015; Kanafin et al., 2022). When designing a new wastewater treatment technology, a common debate is to what extent the pollutants should be removed, when weighing against the potential impacts incurred from the resource consumption (e.g. electricity, chemicals) by this new technology.

In this context, Life Cycle Assessment (LCA) can contribute to evaluating the environmental performance of these technologies, by allocating the environmental impacts across the value chain and by capturing the trade-offs across various categories of environmental concern (Libralato et al., 2012; Tchobanoglous, 2003; Brown et al., 2010; Tchobanoglous et al., 2004; Ho and Martin, 2006; Bustillo-Lecompte and Mehrvar, 2017; Gerbens-Leenes et al., 2013; Davarnejad and Nasiri, 2017; Jensen et al., 2015; Del Nery et al., 2007; Liu et al., 2015; Aziz et al., 2019; Gutu et al., 2021; Musa and Idrus, 2021; Ahmed et al., 2022; Deng and Zhao, 2015; Kanafin et al., 2022; Chung et al., 2008). Corominas et al. (2020) have provided a practical guide on LCA of wastewater treatment systems at different levels. However, the number of published studies of the environmental performance assessment of slaughterhouse wastewater treatment is limited, and due to the wide range of technologies that can be used, it is difficult to perform a comprehensive comparison. Indicatively, Wang et al. (2021) performed a cradle-to-grave life-cycle assessment to estimate the energy depletion and the carbon footprint of slaughterhouse waste treatment using anaerobic digestion. Similarly, Sinsuw et al. (2023) assessed the environmental benefits of the use of a two-stage anaerobic biogas plant for the treatment of slaughterhouse waste, using a set of five midpoint indicators (global warming, acidification, eutrophication, human toxicity and photochemical oxidation potential). Both studies highlighted the environmental benefits of the proposed treatment options with the simultaneous energy production. Çetinkaya and Bilgili used the four endpoint indicators to assess an ultrafiltration membrane as an alternative treatment option. The results have shown that a reduction of approximately 95% has been achieved for BOD and COD (Çetinkaya and Bilgili, 2022).

At planning and design levels, LCA allows the analysis of alternative wastewater management strategies, conceptual designs, and long-term scenarios, and supports the decision-making process for technology development, through a comparison with the existing configuration. At this level, several other methods, such as process modelling, can complement LCA and facilitate decision-making. This is mostly relevant in the early stages of a project, to assess whether a future investment or upgrade in an existing wastewater treatment system is viable. Applying simulation tools to improve process operation entails two major benefits both in terms of cost savings and through a deeper understanding of the process. As a tool of prediction, simulation offers the opportunity to explore and evaluate alternative types of treatment in a short period. Based on the results obtained from the combination of simulation, optimisation and LCA, companies decide whether it is preferable to continue using legacy systems or opting for a new technology implementation.

The goal of this paper is to model alternative wastewater treatment technologies and assess their performance from an environmental perspective in the context of decentralised wastewater management in a slaughterhouse. Section 2 presents the models and the modelling assumptions of the five selected technologies. It is followed by the Life Cycle Assessment of the no treatment scenario (Scenario 1) and two alternative scenarios (Scenario 2 and Scenario 3, in Section 3, and a brief analysis of the findings in Section 4.

2. Models and methods

In the following sections, the main models and methods used for the simulation and assessment of wastewater treatment technologies are presented. Section 2.1 details the models developed for individual technologies, while Section 2.2 presents the main characteristics of the Process Simulation and Modelling (PSM) Suite, a tool developed to model and simulate different scenarios for the wastewater treatment system. Finally, Section 2.3 presents the steps and assumptions for the Life Cycle Assessment of the three alternative scenarios developed.

2.1. Technology modelling

The following five technologies have been selected as part of the wastewater treatment system, with increasing complexity and removal rates for the key wastewater contaminants:

- Screening
- Coagulation & Flocculation
- Dissolved Air Flotation
- Membrane Bioreactor
- Advanced Oxidation Process

The following sections present the characteristics of each technology, the assumptions made, and the models/equations used to simulate their operation, estimating the concentration of the treated wastewater.

2.1.1. Screening

Screening is used as a preliminary treatment to remove large and coarse particles (rocks, branches, plastics, bottles, rags, etc.), and other debris, whose size is greater than 6 mm. It is accomplished by a specific device with openings of the same or greater size. The fundamental objectives of this step are to ensure the smooth operation of the process equipment by preventing any damages, and to reduce the contamination level of the stream. In this case, a coarse screen is implemented. The removal efficiency of the coarse screening depends significantly on the size of the bar screen opening, which is assumed to be 50 mm. Furthermore, cleaning may be carried out manually or mechanically (Metcalf and Eddy, 2014).

2.1.2. Coagulation & flocculation

Due to the presence of stable particles that need to be destabilised, the wastewater stream may be further treated by coagulation and flocculation using the necessary chemicals. Chemical coagulation is the process of destabilising colloidal particles contained in wastewater by adding coagulants. The particles' size ranges from 0.01 to 1 μm. These particles are usually negatively charged with strong repelling forces between them. Water molecules of relatively small size surround them, randomly leading to the Brownian motion, which keeps them in suspension. Coagulants adsorb onto the desired compounds resulting in the decrease of the repelling forces. This way, the particle collisions are favoured. The destabilisation leads to the attachment of colloidal particles to others and thus to the formation of larger particles. Hence, this

way, particle growth during the flocculation process becomes easier (Metcalf and Eddy, 2014). The concentration of the coagulant is an important factor in the process efficiency (Baruth, 2005).

Flocculation follows the process of particles' destabilisation and is categorised into microflocculation and macroflocculation. The former refers to the particles' aggregation of size 0.001–1 μm, caused by the random Brownian motion of the molecules. The latter describes the aggregation of particles of size greater than 1–2 μm, caused by the induced velocity gradient or differential settling. Flocculants may be added to enhance the process efficiency helping in the formation of particles that can settle (Metcalf and Eddy, 2014; Baruth, 2005).

Coagulation and flocculation are widely applicable in the industry. The removal percentage of suspended solids and heavy metals depends on the temperature, pH and coagulant dosage (Amin et al., 2021). The concentration of the chemicals was selected based on indicated literature values (Ehteshami et al., 2015). The duration of the process is also an important factor (Nnaji et al., 2014). It is assumed that wastewater consists of monodisperse particles. Coagulation process model follows first-order kinetics to predict the concentration of the particles at the effluent, C (mg/L). It depends on the operation time, t (s), and the first-order rate constant, k (1/min) (Mageshkumar and Karthikeyan, 2015).

$$dC/dt = -k \cdot C \tag{1}$$

The rate constant of the coagulation process depends on the collision efficiency, E (dimensionless), and the Smoluchowski rate constant for rapid coagulation, K_R (1/min). The latter is calculated based on the Boltzmann constant, k_B ($m^2 \cdot kg/s^2/K$), temperature, T (K), and viscosity, μ (Pa•s).

$$k = E \cdot K_R \tag{2}$$

$$K_R = 4 \cdot k_B \cdot T/(3 \cdot \mu) \tag{3}$$

In addition, the Brownian diffusion coefficient, D ($kg^2/m/s$), and the friction factor are calculated by Eqs. (4) and (5), respectively (Precious Sibiya et al., 2021).

$$D = k_B \cdot T/\beta \tag{4}$$

$$\beta = 2 \cdot k \tag{5}$$

Due to aggregation of the colloidal matter, it is necessary to estimate the concentration of particles at the effluent after 30 min. The kernel was assumed to be constant, resulting in the following expression for the number concentration:

$$N_n(t)/N_o = (k \cdot N_o \cdot t/2)^{n-1} \cdot (1 + (k \cdot N_o \cdot t/2))^{-(n+1)} \tag{6}$$

where $N_n(t)$ is the effluent concentration of the particles at time t and N_o is the initial concentration of the particles. Eq. (6) is applied for monomers (n = 1), dimers (n = 2), trimmers (n = 3) or for higher order particles. The efficiency of this process, R (%), is determined by Eq. (7) (Nnaji et al., 2014):

$$R = 100\ (\ N_o - N_n(t))\ /\ N_o \tag{7}$$

The energy requirements, E (kWh), are calculated as a function of power requirements, P (kW), and operation time, t (h):

$$P = G^2 \cdot \mu \cdot V \tag{8}$$

$$E = P \cdot t \tag{9}$$

Where G is the velocity gradient (1/s), μ is the dynamic viscosity (kg/m/s), and V is the volume (m^3).

2.1.3. Dissolved air flotation (DAF)

Dissolved air flotation accomplishes the clarification of industrial wastewater by separating the solid particles from a liquid medium, utilizing air bubbles. Two distinct zones are formed in the air flotation tank, the contact zone and the separation zone. Inside the first compartment, the air is supplied through the recycle stream under pressure, aiming at forming air bubbles that attach onto the surface of flocculated particles or collide with them, resulting in floc-bubbles aggregates. Consequently, free bubbles, floc-bubbles aggregates and unattached flocculated particles are moving to the second compartment, the separation zone. The first two components rise to the surface, representing the float layer that will be skimmed, in contrast with the unattached floc particles that settle on the bottom and will be collected along with the clarified effluent stream (Edzwald, 2010; Gkika et al., 2022). Earlier studies have tried to model the overall performance of the dissolved air flotation (Palaniandy et al., 2017; Behin and Bahrami, 2012; Jung et al., 2006). In this paper, the population balance model is adopted to model the contact zone efficiency and is, therefore combined, with the rise velocity of the floc-bubbles agglomerates for the modelling of the overall process.

Assuming that flocs have been formed during the flocculation process, their size remains constant. The agglomerates' size (i.e. diameter, d_{agglo}) and density (ρ_{agglo}) are important parameters that are calculated by Eqs. (10) and (11), respectively.

$$d_{agglo} = (d_p^3 + d_b^3)^{1/3} \tag{10}$$

$$\rho_{agglo} = (\rho_p \cdot d_p^3 + i \cdot \rho_b \cdot d_b^3) \cdot (d_p^3 + i \cdot d_b^3)^{-1} \tag{11}$$

where d_p is the diameter of flocs (m), d_b is the diameter of air bubbles (m), ρ_p is the density of flocs (kg/m^3), ρ_b is the density of air bubbles (kg/m^3), and i is the number of attached bubbles on one floc (dimensionless). The collisions between flocs and air bubbles occur due to turbulent mixing with intensity, G (1/s), which is calculated based on the turbulent dissipation of energy, ε (W/m^3), and viscosity, μ_w (Pa•s):

$$G = (\varepsilon / \mu_w)^{1/2} \tag{12}$$

Also, the density of the air bubbles supplied in the first compartment of the flotation tank depends on the molecular weight of air, MW_{air} (g/mol), atmospheric pressure, p_{atm} (Pa), density, ρ_w (kg/m^3), gravitational constant of acceleration, g (m/s^2), contact zone height, H_{cz} (m), gas constant, R ($Pa \bullet m^3/mol/K$), and temperature T (K). It is given by:

$$\rho_p = MW_{air} \bullet (p_{atm} + \rho_w \bullet g \bullet H_{cz}) \bullet (R \bullet T)^{-1} \tag{13}$$

The rise velocity of the floc-bubble agglomerates, u_{agglo} (m/s), is affected by numerous factors, including the diameter and the density of air bubbles and flocs, the viscosity, and the detention time in the contact zone, t_{CZ} (s). The buoyancy force applied on the flocs-air bubbles agglomerates, F_b (N), is required for the calculation of their rise velocity.

$$F_b = \pi \bullet d_{agglo}^{\ 3} \bullet (\rho_w - \rho_{agglo}) \bullet g / 6 \tag{14}$$

Furthermore, the Reynolds number of the flow of the formed agglomerates is given by Eq. (15):

$$Re = \rho_w \bullet u_{agglo} \bullet d_{agglo} / \mu \tag{15}$$

Except for the buoyancy force, floc-air bubbles agglomerates receive the drag force, F_d (N), which is calculated based on the drag coefficient of a sphere, C_D (dimensionless) (Jung et al., 2006).

$$F_d = 8 \bullet C_D / (\pi \bullet \rho_w \bullet u_{agglo}^2 \bullet d_{agglo}^2) \tag{16}$$

However, the calculation of the drag coefficient depends on the Reynolds number. Specifically, there are three alternatives (Green and Southard, 2019):

$$C_D = 24 / Re,\ Re < 0{\cdot}1$$

$$C_D = (24 / Re) \bullet (1 + 0{\cdot}14 \bullet Re^{0{\cdot}7}),\ 0{\cdot}1 < Re < 10^4 \tag{17}$$

$$C_D = 0{\cdot}19 - (80000 / Re),\ Re > 10^6$$

When the buoyancy force and the drag force are even, the rise velocity of the agglomerates is estimated by Eq. (18), using an initial value provided by Eq. (19) with Stokes approximation, which corresponds to Reynolds number tending to infinity.

$$u_{agglo} = ((8 \bullet F_b) / (C_D \bullet \pi \bullet \rho_w \bullet d_{agglo}^2))^{1/2} \quad (18)$$

$$u_{agglo,\ initial} = (\rho_w - \rho_{agglo}) \bullet d_{agglo}^2 \bullet g / (18 \bullet \mu_w) \quad (19)$$

The maximum number of the attached bubbles on a floc is determined by i_{max}.

$$i_{max} = c(d_p/d_b)^2 \quad (20)$$

Where c a numerical constant. It has been proposed by (Matsui et al., 1998) that c = 1. A population balance model is used for predicting the number of flocs with attached i-bubbles, n_i, using as initial value at time t = 0 s the n_o.

$$dn_o/dt = - k \bullet \alpha_o \bullet n_o \bullet n_{bubbles}, \text{ when } i = 0 \quad (21)$$

$$dn_i/dt = k \bullet \alpha_{i-1} \bullet n_{i-1} \bullet n_{bubbles} - k \bullet \alpha_i \bullet n_i \bullet n_{bubbles}, \text{ when } i = 1\text{-}i_{max} \quad (22)$$

Where k is the turbulent collision rate constant and $n_{bubbles}$ the number of bubbles per unit volume in the contact zone of the dissolved air flotation tank.

$$k = a \bullet G \bullet (d_p + d_b)^3 \quad (23)$$

$$n_{bubbles} = 6 \bullet \Phi_b / (\pi \bullet d_b^3) \quad (24)$$

Where a is a numerical constant representing the ratio of flocs size and bubble size as well as the number of attached bubbles, and Φ_b is the air bubble volume concentration (mg/L), which is calculated by:

$$\Phi_b = C_b / \rho_b \quad (25)$$

The mass concentration of bubbles in the contact zone, C_b (mg/L), is calculated based on a mass balance under steady-state conditions.

$$C_b = ((e\ (C_r - C_{s,air})\ R) - k)\ (1+R)^{-1} \quad (26)$$

Where C_r is the amount of air that will precipitate based on saturation of air in the recycle stream theoretically, $C_{s,air}$ the amount of air in the influent stream, e is the air efficiency factor, R represents the recycle stream, and k refers to air deficit in the influent stream. Furthermore, the adhesion efficiency (α_i) depends on the number of attached bubbles and is expressed by Eqs. (27) or (28).

$$\alpha_i = \alpha_o\ (1 - i \bullet d_b^2/d_p^2),\ i = (1,\ i_{max} - 1) \quad (27)$$

$$\alpha_i = 0,\ i = i_{max} \quad (28)$$

Hence, the system of the following differential equations needs to be solved, in order to estimate the number of flocs with attached bubbles, and thus the removal efficiency of the dissolved air flotation (Edzwald, 2010; Jung et al., 2006):

$$dn_o/dt = - 6 \bullet a \bullet G \bullet (d_p+d_b)^3 \bullet \Phi_b \bullet \alpha_o \bullet n_o \bullet (\pi \bullet d_b^3)^{-1}, i=0$$

$$dn_i/dt = 6 \bullet a \bullet G \bullet (d_p+d_b)^3 \bullet \Phi_b \bullet (\pi \bullet d_b^3)^{-1} \bullet ((1 - (i\text{-}1) \bullet d_b^2 \bullet d_p^{-2}) n_{i-1} - (1 - i \bullet d_b^2 \bullet d_p^{-2}) n_i),\ i = (1,\ i_{max}\text{-}1) \quad (29)$$

$$dn_{imax}/dt = 6 \bullet a \bullet G \bullet (d_p+d_b)^3 \bullet \Phi_b \bullet (\pi \bullet d_b^3)^{-1} \bullet (1 - (i_{max}\text{-}1) \bullet d_b^2 \bullet d_p^{-2}) \bullet n_{imax-1},\ i = i_{max}$$

The energy requirements for the DAF, E_{DAF} (kWh), depend on the saturator gauge pressure, p (kPa), the volume, V (m^3), and the operation time, t (h). The pressure was 500 kPa based on literature (Edzwald, 2010).

$$E_{DAF} = p \bullet V \bullet t \quad (30)$$

2.1.4. Membrane bioreactor

Coagulation-flocculation and dissolved air flotation are two of the most common physicochemical methods used for the wastewater treatment in a slaughterhouse. However, further treatment is required due to insufficient COD removal (Gautam et al., 2023), with the membrane bioreactor (MBR) being a usual choice. It consists of the biological unit and the membrane module, aiming at the recovery of resources from the wastewater. The membrane achieves the separation of solids and the retention of bacteria, resulting in the production of a clarified stream. Overall, the membrane is used as a barrier due to removal of suspended, colloidal and dissolved matter. The operation mode may be either dead-end or cross-flow. The former results in the permeate production, while the latter includes both a permeate and a retentate stream. In addition, turbidity, COD and nitrogen levels decrease, in case an anoxic zone is included in the MBR (Hai et al., 2014a).

Many researchers have engaged with the MBR modelling (Deowan et al., 2019; Nelson et al., 2019; Gulhan et al., 2022; Lindamulla et al., 2021). In this paper, the membrane bioreactor is assumed to consist of an anoxic zone followed by an aerobic one. It is assumed that it is a continuously stirred-tank reactor with an integrated ultrafiltration membrane. Hence, it is an internal submerged membrane bioreactor. For the MBR modelling the Activated Sludge Model 1 (ASM1) was used, which was introduced by (Henze et al., 2002). In this regard, mass balances based on the ASM1 under steady-state conditions are formulated. The process variables of the MBR model can be found in the Appendix (Table A1).

The temperature is considered constant, allowing the use of invariable kinetic parameters. The correction factors for denitrification (η_g, η_h) and the coefficients related to the nitrification are also assumed constant. The hydrolysis rate of the soluble biomass is considered to be equal to the hydrolysis rate of the biomass derived from the degradation. The aeration process has been modelled, with an internal recycle stream from the aeration tank to the anoxic one, r_{int} (dimensionless), and a membrane recirculation ratio, r_{mr} (dimensionless). The system of ordinary differential equations (ODEs) that will be considered, and will allow estimating the removal ratio of the contaminants, is presented in Table 1 (Nelson et al., 2019; Lindamulla et al., 2021; Henze et al., 2002; Judd et al., 2011).

The flow rate of the influent stream is expressed as Q_{in} (m^3/d), and

Table 1
ODEs for the membrane bioreactor simulation.

$dS_S/dt = (Q_{in}/V) \bullet (S_{S,in}\text{-}S_S) - \mu_{\mu\alpha\chi,H} \bullet M_2 \bullet (M_{8\ h} + I_8 \bullet M_9 \bullet \eta_g) \bullet Y_H^{-1} \bullet X_{B,H} + k_h \bullet k_{sat} \bullet (M_{8\ h} + I_8 \bullet M_9 \bullet \eta_h) \bullet X_{B,H}$	(31)
$dX_S/dt = (Q_{in}/V) \bullet (X_{S,in}\text{-}X_S) + (Q_R/V) \bullet (b\text{-}1) \bullet X_S + (1\text{-}f_p) \bullet (b_H \bullet X_{B,H} + b_A \bullet X_{B,A}) - k_h \bullet k_{sat} \bullet (M_{8\ h} + I_8 \bullet M_9 \bullet \eta_h) \bullet X_{B,H}$	(32)
$dX_{B,H}/dt = (Q_{in}/V) \bullet (X_{B,H,in}\text{-}X_{B,H}) + (Q_R/V) \bullet (b\text{-}1) \bullet X_{B,H} + \mu_{max,H} \bullet M_2 \bullet M_{8\ h} \bullet X_{B,H} + \mu_{max,H} \bullet M_2 \bullet I_8 \bullet M_9 \bullet \eta_g \bullet X_{B,H} - b_H \bullet X_{B,H}$	(33)
$dX_{B,A}/dt = (Q_{in}/V) \bullet (X_{B,A,in} - X_{B,A}) + (Q_R/V) \bullet (b\text{-}1) \bullet X_{B,A} + \mu_{max,A} \bullet M_{10} \bullet M_{8a} \bullet X_{B,A} - b_A \bullet X_{B,A}$	(34)
$dS_O/dt = (Q_{in}/V) \bullet (S_{O,in}\text{-}S_O) + K_{LA} \bullet (S_{O,max}\text{-}S_O) - (1\text{-}Y_H) \bullet (Y_H)^{-1} \bullet \mu_{max,H} \bullet M_2 \bullet M_{8\ h} \bullet X_{B,H} - (4.57\text{-}Y_A)(Y_A)^{-1} \bullet \mu_{max,A} \bullet M_{10} \bullet M_{8a} \bullet X_{B,A}$	(35)
$dS_{NO}/dt = (Q_{in}/V) \bullet (S_{NO,in}\text{-}S_{NO}) - (1\text{-}Y_H) \bullet (2.86 \bullet Y_H)^{-1} \bullet \mu_{max,H} \bullet M_2 \bullet I_8 \bullet M_9 \bullet \eta_g \bullet X_{B,H} + (Y_A)^{-1} \bullet \mu_{max,A} \bullet M_{10} \bullet M_{8a} \bullet X_{B,A}$	(36)
$dS_{NH}/dt = (Q_{in}/V) \bullet (S_{NH,in}\text{-}S_{NH}) - i_{XB} \bullet \mu_{max,H} \bullet M_2 \bullet (M_{8\ h} + I_8 \bullet M_9 \bullet \eta_h) \bullet X_{B,H} - (i_{XB} + 1/Y_A) \bullet \mu_{max,A} \bullet M_{10} \bullet M_{8a} \bullet X_{B,A} + k_A \bullet S_{ND} \bullet X_{B,H}$	(37)
$dS_{ND}/dt = (Q_{in}/V) \bullet (S_{ND,in}\text{-}S_{ND}) - k_A \bullet S_{ND} \bullet X_{B,H} + k_h \bullet k_{sat} \bullet (M_{8\ h} + I_8 \bullet M_9 \bullet \eta_h) \bullet X_{B,H} \bullet X_{ND} \bullet X_S^{-1}$	(38)
$dX_{ND}/dt = (Q_{in}/V) \bullet (X_{ND,in} - X_{ND}) + (Q_R/V) \bullet (b\text{-}1) \bullet X_{ND} + (i_{XB}\text{-}f_p \bullet i_{XP}) \bullet (b_H \bullet X_{B,H} + b_A \bullet X_{B,A}) - k_h \bullet k_{sat} \bullet (M_{8\ h} + I_8 \bullet M_9 \bullet \eta_h) \bullet X_{B,H} \bullet X_{ND} \bullet X_S^{-1}$	(39)
$dS_I/dt = (Qin/V) \bullet (S_{I,in} - S_I)$	(40)
$dX_I/dt = (Qin/V) \bullet (X_{I,in} - X_I) + (Q_R/V) \bullet (b\text{-}1) \bullet X_I$	(41)
$dX_P/dt = (Qin/V) \bullet (X_{p,in} - X_p) + (Q_R/V) \bullet (b\text{-}1) \bullet X_p + f_p \bullet b_H \bullet X_{B,H} + f_p \bullet b_A \bullet X_{B,A}$	(42)
Where the aforementioned reaction rates are:	
$M_2 = S_S \bullet (K_S + S_S)^{-1}$	(43)
$M_{8a} = S_O \bullet (K_{O,A} + S_O)^{-1}$	(44)
$M_9 = S_{NO} \bullet (K_{NO} + S_{NO})^{-1}$	(45)
$M_{10} = S_{NH} \bullet (K_{NH} + S_{NH})^{-1}$	(46)
$I_8 = K_{O,H} \bullet (K_{O,H} + S_O)^{-1}$	(47)
$k_{sat} = X_S \bullet (K_X\ X_{B,H} + X_S)^{-1}$	(48)

the total reactor volume as V (m^3). Assuming that the membrane retains all the particulate matter, the concentrating factor is defined by the recycle ratio, R (dimensionless), and the wasted fraction, w_1 (dimensionless):

$$b = (1 + R)\bullet(R + w_1)^{-1} \quad (49)$$

The total COD in the influent stream comprises of S_S, S_i, X_S, and X_I (Gautam et al., 2023). The total nitrogen (TN) consists of several process variables, as expressed by Eq. (50) (Nelson et al., 2019).

$$TN = S_{NO} + S_{NH} + S_{ND} + X_{ND} + i_{XB}\bullet(X_{B,H} + X_{B,A}) + i_{XP}\bullet(X_P + X_I) \quad (50)$$

Table A2 (in the Appendix) illustrates all the kinetic and stoichiometric parameters used for the modelling and simulation of the membrane bioreactor (Nelson et al., 2019; Henze et al., 2002; Nelson and Sidhu, 2009).

Among the most important parameters for MBR is the food-to-microorganism ratio, F/M (g COD/ g VSS/d), expressed as:

$$F/M = (Q_{in}\bullet S_O) / (V_{aer}\bullet MLSS) \quad (51)$$

Where V_{aer} is the aeration tank volume and MLSS represents the mixed liquor suspended solids within the reactor (mg/L). A lower F/M leads to a higher removal efficiency of the substrate, due to higher utilisation rate of the substrate by the microorganisms. Another modelled process parameter is the hydraulic retention time, HRT (h), which is estimated by dividing the volume reactor with the influent flow rate.

The aerobic conditions within the reactor are ensured through air supply, which serves as the oxidising agent of the biodegradable organic matter and ammonia. In addition, it contributes to the endogenous respiration of microorganisms. In this regard, the produced biomass, $P_{x,bio}$ (kg/d), during the process can be calculated by Eq. (52).

$$P_{x,bio} = Q_{in}\bullet Y_H\bullet(S_O\text{-}S)\bullet(1 + b_H\bullet SRT)^{-1}\bullet 10^{-3} + f_d\bullet b_H\bullet Q_{in}\bullet Y_H\bullet(S_O\text{-}S)\bullet 10^{-3}\bullet SRT\bullet(1 + b_H\bullet SRT)^{-1} \quad (52)$$

Hence, the required oxygen through air supply, R_O (kg/d), is modelled as:

$$R_O = Q_{in}\bullet(S_O\text{-}S)\bullet 10^{-3} - 1{\cdot}42\bullet P_{x,bio} + 4{\cdot}57\bullet Q_{in}\bullet NO_x\bullet 10^{-3} \quad (53)$$

Where S_O is the soluble oxygen concentration in the influent stream (mg/L), S is the substrate concentration in the outlet stream (mg/L), SRT is the sludge retention time (d), and NO_x is the produced amount of nitrates during nitrification (Metcalf and Eddy, 2014; Hai et al., 2014b). This way, air flow rate, M_O (m^3/h), is modelled based on the required oxygen:

$$M_O = R_O \bullet (24 \bullet \rho_{air})^{-1} \quad (54)$$

Where ρ_{air} is the air density, which was assumed to be 1.2 kg/m^3 (Yilmaz et al., 2023). Energy is required for mixing (E_{mix}), recirculation within the reactor (E_{rec}), air supply and air scour for permeate (E_{air}) and sludge separation (E_w), whose estimation is given by the following equation (Kanafin et al., 2022; Nelson et al., 2019).

$$E_{MBR} = (E_{mix} + E_{rec} + E_{air}) \bullet Q_{in} \bullet t + E_w \bullet Q_w \bullet t \quad (55)$$

Where Q_w is the flow rate of sludge (m^3/h) and t is the operation time (h). For the simulation literature data were used, as 0.04 kWh/m^3 for mixing, 0.016 kWh/m^3 for recirculation, 0.006 kWh/m^3 for air supply, 0.32 kWh/m^3 for air scour, and 0.0004 kWh/m^3 for sludge separation (Hai et al., 2014a).

2.1.5. Advanced oxidation process

Toxic and recalcitrant organic contaminants must be treated with an advanced oxidation process, including the use of ultraviolet light and hydrogen peroxide (UV/H_2O_2). In this regard, the photolysis of the hydrogen peroxide due to ultraviolet radiation results in the formation of hydroxyl radicals (Rubio-Clemente et al., 2017). Hence, the cleavage of the O-O bond triggers a series of chemical reactions, as shown in Table A3 (Pandis et al., 2022). Among the advantages of this process are the almost complete mineralisation of the refractory contaminants and a lack of sludge production. Also, it is an environmentally friendly technology, which leads to the production of non-toxic compounds (Manna and Sen, 2022). The factors affecting the process comprise the initial concentration of hydrogen peroxide, as it is the oxidant, initial concentration of the contaminants, pH of the solution, temperature, time, and the wastewater composition (Hassaan et al., 2022; Liu et al., 2020). The type of the UV lamp, UV light transmittance of the quartz sleeve, optical path length, and the optical properties of the wastewater play an important role in the performance of the advanced oxidation process using UV and H_2O_2 (Ameta and Ameta, 2018).

The concentration profile of the hydrogen peroxide can be predicted based on Beer-Lambert law, the definition of the quantum yield, φ_{H2O2} (mol/Ein), and taking into account the involved reactions.

$$dH_2O_2/dt = -\varphi_{H2O2}\bullet I_{H2O2} - (2{\cdot}7\bullet 10^7\bullet C_{H2O2}\bullet C^{\bullet}_{HO}) - (3{\cdot}0\bullet C_{H2O2}\bullet C^{\bullet}_{HO2}) - (0{\cdot}13\bullet C_{H2O2}\bullet C^{\bullet-}_{O2}) + (5{\cdot}5\bullet 10^9\bullet C^{\bullet}_{HO}\bullet C^{\bullet}_{HO}) + (8{\cdot}6\bullet 10^5\bullet C^{\bullet}_{HO2}\bullet C^{\bullet}_{HO2}) - (4{\cdot}3\bullet 10^5\bullet C_{H2O2}\bullet C^{\bullet-}_{CO3}) - (2{\cdot}7\bullet 10^7\bullet C_{H2O2}\bullet C^{\bullet-}_{HPO4}) - (1{\cdot}2\bullet 10^7\bullet C_{H2O2}\bullet C^{\bullet-}_{SO4}) - (0{\cdot}025\bullet C_{H2O2}) + (1{\cdot}0\bullet 10^{10}\bullet C^{\bullet}_{HO2}\bullet C^{+}_{H}) \quad (56)$$

The UV-radiation intensity absorbed by hydrogen peroxide, I_{H2O2} (Ein/L/s), is calculated using the applied UV light intensity, I_o (Ein/s), the fraction of the UV-radiation absorbed by this component, f_{H2O2} (dimensionless), optical path length, b (cm), and molar extinction coefficient of all light-absorbing species, ε_{H2O2} for H_2O_2, ε_{NO3}^- for NO_3^-, and ε_{TOC} for TOC (L/mol/cm). For example, the UV-radiation intensity absorbed by hydrogen peroxide is determined by Eq. (57).

$$I_{H2O2} = I_o\bullet f_{H2O2}\bullet[1\text{-}\exp(-2{\cdot}3\bullet b\bullet(\varepsilon_{H2O2}\bullet C_{H2O2} + \varepsilon^-_{NO3}\bullet C_{NO3\text{-}} + \varepsilon_{TOC}\bullet C_{TOC}))] \quad (57)$$

It should be mentioned that the calculation of the fraction of the UV-radiation absorbed by each species is influenced by the other light-absorbing species.

$$f_{H2O2} = (\varepsilon_{H2O2}\bullet C_{H2O2})\bullet(\varepsilon_{H2O2}\bullet C_{H2O2} + \varepsilon^-_{NO3}\bullet C_{NO3\text{-}} + \varepsilon_{TOC}\bullet C_{TOC})^{-1} \quad (58)$$

$$f_{NO3\text{-}} = (\varepsilon^-_{NO3}\bullet C^-_{NO3})\bullet(\varepsilon_{H2O2}\bullet C_{H2O2} + \varepsilon^-_{NO3}\bullet C_{NO3\text{-}} + \varepsilon_{TOC}\bullet C_{TOC})^{-1} \quad (59)$$

$$f_{TOC} = (\varepsilon_{TOC}\bullet C_{TOC})\bullet(\varepsilon_{H2O2}\bullet C_{H2O2} + \varepsilon^-_{NO3}\bullet C_{NO3\text{-}} + \varepsilon_{TOC}\bullet C_{TOC})^{-1} \quad (60)$$

The concentration profiles of the wastewater components were obtained likewise by implementing non-pseudo-steady state conditions, solving a complex system of differential equations derived from the rate constants of Table A3 (Yilmaz et al., 2023).

For the simulation of the advanced oxidation process, the following assumptions were made. Hydrogen peroxide, organic contaminants, and nitrate ions are the only light-absorbing species in the wastewater. However, nitrate ions absorb the UV light at this wavelength, i.e. 254 nm, with a low quantum yield (Glaze et al., 1995; Park et al., 2014). $CO_3^{\bullet-}$ species are assumed to be scavengers of hydroxyl radicals and superoxide radicals. Also, they react with the hydrogen peroxide and the conjugate base. Their weak oxidising properties make their contribution to the organics oxidation negligible (Crittenden et al., 1999). Furthermore, specific inorganic ions, including bicarbonates, hydrogen phosphate, dihydrogen phosphate, hydrogen sulphate, nitrites, and peroxynitrite are scavengers of hydroxyl radicals (Ismail et al., 2018). On the contrary, sulphate, phosphate and nitrate ions do not react with the hydroxyl radicals (Grebel et al., 2010). Overall, the mineralisation of the organic matter is a result of direct photolysis and oxidation by the hydroxyl radicals (Glaze et al., 1995; Bustillo-Lecompte et al., 2016). Regarding the by-products derived from the oxidation of the organics, they have not been taken into account in the modelling. The optical path length was assumed to be 6.35 cm and the applied UV light intensity 0.00002 Ein/L/s. The molar extinction coefficients for H_2O_2, NO_3^-, and TOC were set at 18.7, 3.0, and 132.7 L/mol/cm, respectively (Rubio-Clemente et al., 2017; Bustillo-Lecompte et al., 2016; Mack and Bolton,

1999) and the duration was set at 30 min. To calculate the energy requirements, E_{AOP} (kWh), an 0.014 kW low pressure UV lamp was assumed (Bustillo-Lecompte et al., 2016).

$$E_{AOP} = P \bullet t \quad (61)$$

Where P is the power of the lamp and t is the irradiation time.

2.2. Alternative treatment scenarios

Process Simulation and Modelling (PSM) Suite is the key to model and simulate all the water and wastewater treatment technologies. The industrial production system is represented in the PSM as a material flow network (MFN) in which flows of resources (wastewater, water, chemicals, energy, air, and sludge) are included. The technologies are represented as processes, which are directly linked with the physical flows of resources. All the processes and the flows of the system are modelled into MFN, building the various scenarios of the flow model (Mack and Bolton, 1999). The PSM Suite enables the prediction of the effluent quality, the energy requirements and the chemicals consumption as well.

Three different scenarios have been modelled using the PSM suite. Scenario 1 is the baseline scenario, which represents the disposal of untreated wastewater, without the involvement of any treatment technologies. Scenario 2 represents the wastewater treatment system selected to reduce the contaminant load, using coagulation, flocculation and dissolved air flotation (Fig. 1), before being discharged to the river. Scenario 3 represents the wastewater treatment system selected to reduce the contaminant load to an appropriate level for safe reuse in the plant. It is assumed that 30% of the treated wastewater will be reused on-site, for industrial and non-drinking purposes, while the rest will be discharged to the river. The technologies involved in this scenario include those of Scenario 2 together with a membrane bioreactor and an advanced oxidation process (Fig. 2).

2.3. Life cycle assessment

A Life Cycle Assessment has been performed to assess the environmental impact of these three scenarios. The methodological approach used to carry out the research followed the Life Cycle Assessment framework, as detailed in the ISO14040/44:2006, and included the following four steps:

- Goal and Scope Definition, i.e. the definition of the study objective and the selected system boundaries (both spatial and temporal).
- Life Cycle Inventory (LCI), i.e. formulation of a representative list of all inlet and outlet flows that the system exchanges with the environment.
- Life Cycle Impact Assessment (LCIA), i.e. calculation of the environmental impact indicators based on the inventory flows and the corresponding characterisation factors.
- Interpretation of results.

The Life Cycle assessment was performed using SimaPro 9.2 Academic License and the most recent version (3.9) of the ecoinvent database.

2.3.1. Goal and scope definition

The goal of the LCA is to compare the environmental performance of the three alternative wastewater treatment scenarios, where the system boundaries are illustrated in Fig. 3. A volume-based unit is the most common functional unit in the LCA of wastewater treatment and, for this study, 1 m^3 of wastewater effluent prior to entering the wastewater treatment system is chosen. The focus of the study was the operational Life Cycle Assessment on the water line, which implies that the design, building and maintenance of different process equipment have not been included. This is supported by the findings of Ding et al., who have done a literature review on different system boundaries of WWTPs and 31 out of 37 relevant studies have shown that the construction and dismantlement of WWTPs make only a negligible impact relative to their operations, especially for long term technical system (Ding et al., 2021; Lombardi et al., 2017; Johansson et al., 2008).

2.3.2. Life cycle inventory (LCI)

The foreground LCI for Scenario 1 was compiled directly from experimental data, whose composition is described in Table 5. These data are compared to other slaughterhouse wastewater characteristics reported in previous studies, which are summarised in Table 2.

The foreground LCI for Scenario 2 is based on both lab scale experiments and modelling output, and that for Scenario 3 is based in its entirety on modelling outputs. Within the scope of this study, the inventory data include power consumption, chemicals consumption, solid waste disposal, and emission of effluents, as illustrated in the next section.

The background LCI was populated using the ecoinvent LCI database,

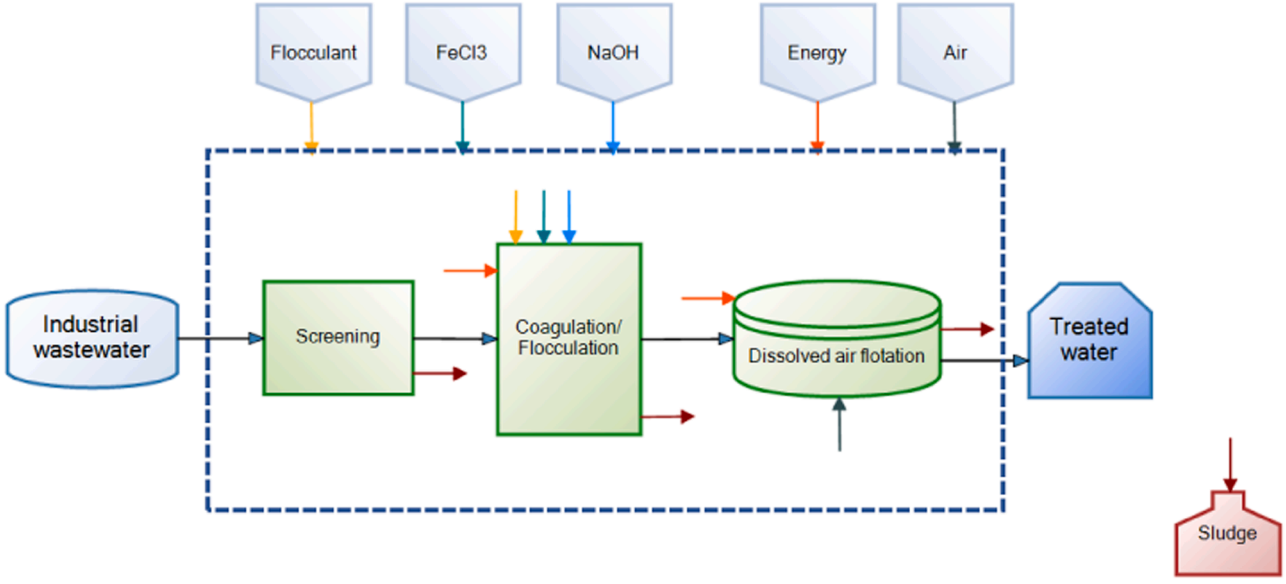

Fig. 1. Process flow diagram of Scenario 2 in the PSM suite.

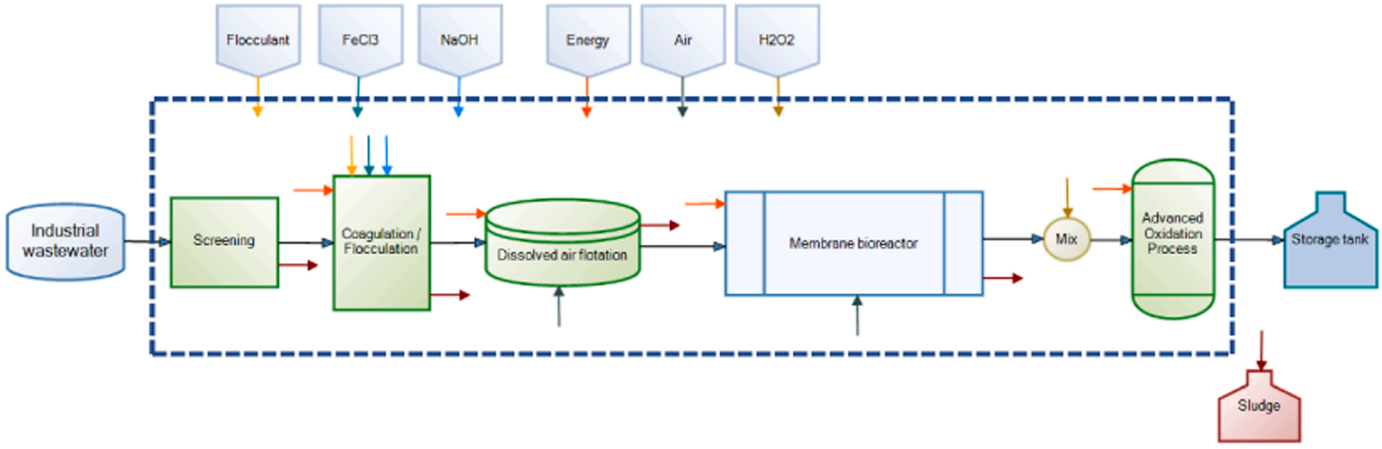

Fig. 2. Process flow diagram of Scenario 3 in the PSM suite.

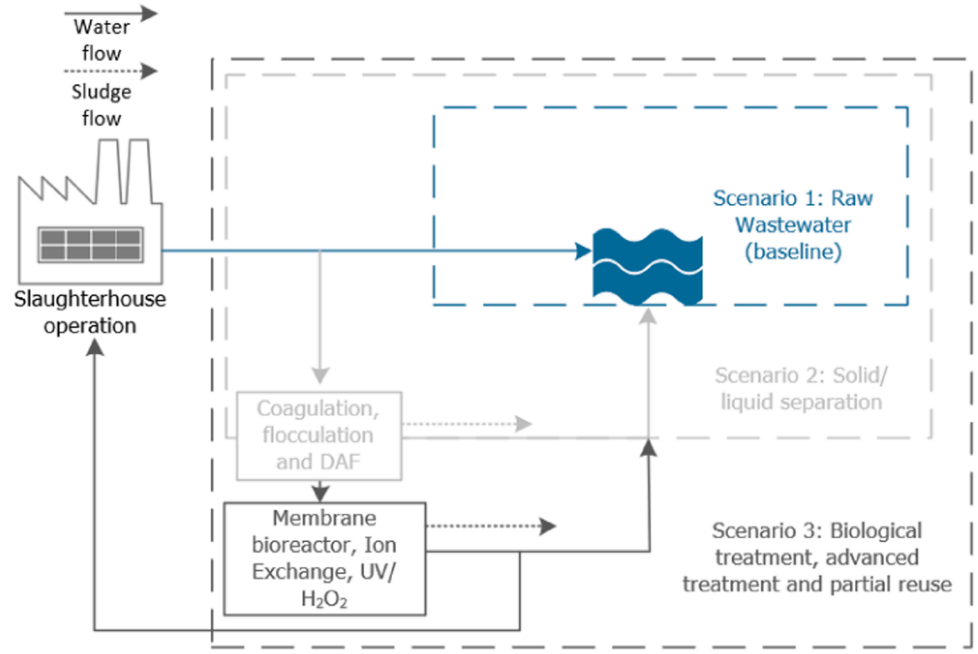

Fig. 3. Scope and system boundary of this study.

as implemented in SimaPRO. The selection of these data was done on a hierarchical approach whereby Europe average will be selected whenever available, followed by Switzerland and lastly rest of world, when the above two data sets are not available. In terms of chemical consumption, no chemicals were generated on site and thus all the chemicals were modelled as market readily available products, accounting for the environmental impact of the production of these chemicals from a life cycle perspective. The energy consumption of the processes is assumed to be electricity purchased from the national grid station, in medium voltage level between 1 kV and 24 kV, which is the main source of power typically used for medium sized industry.

2.3.3. *Life cycle impact assessment*

The Environmental Footprint (EF) impact assessment method has been selected for the impact assessment of the alternative scenarios. The EF is an LCA methodology, adopted by the European Commission in the Environmental Footprint transition phase of the commission to incentivise industries manufacturing products with improved environmental performance, based on reliable, verifiable, and comparable information. The method is also foreseen to be applied in the context of European policies and legislations, such as the European Green Deal. This method includes the most important impact categories for wastewater, such as eutrophication potential and freshwater ecotoxicity. The full list of impact categories, considered in this study, is presented in Table 3.

In order to populate the LCI, a series of assumptions have been made, mostly in terms of the characterisation of effluent streams, certain components of which are not included in the ecoinvent database. Characterisation is the process of linking the environmental pressures represented by inventory data to individual impact category and quantifying the impact magnitude.

The characterisation factor for waterborne COD and BOD is currently unavailable for the EF inventory analysis and thus a correction factor based on another impact assessment method was used (EU Commission, 2023). The environmental impact of COD and BOD is modelled as phosphate equivalent in accordance with the CML Impact assessment method, whereby 1 kg of COD or BOD (expressed as O_2) is equivalent to 0.022 kg of phosphate in PO_4^{3-} (i.e. kg PO_4^{3-} eq) or approximately 0.00452 kg of phosphorus equivalent (i.e. kg P eq) (JRC EU, 2023). A characterisation factor based on CML was chosen because waterborne emissions of dissolved organic compounds (COD, BOD and DOC) were

Table 2
Slaughterhouse wastewater characteristics reported in literature.

Resource	(Amuda and Alade, 2006)	(Aziz et al., 2019)	(Bustillo-Lecompte and Mehrvar, 2015)	(Mkilima, 2022)	(Madeira et al., 2023)	(Rodríguez-Martínez et al., 2002)	(Nacheva et al., 2011)	(Yaakob et al., 2018)
Alkalinity	-	350–1340 g/m^3	-	-	-	530 g/m^3	722–1356 g/m^3	-
pH	6.70	5.00–7.80	6.00–6.90	5.52–7.36	7.10	7.50	7.48–7.69	7.30–8.60
Chemical Oxygen Demand	19945 g/m^3	1100–15000 g/m^3	527–15256 g/m^3	4606–9815 g/m^3	6981 g/m^3	12800 g/m^3	3534–4994 g/m^3	3154–7719 g/m^3
Biological Oxygen Demand	14370 g/m^3	600–3900 g/m^3	200–8231 g/m^3	1270–8542 g/m^3	-	-	-	1341–1821 g/m^3
Total Organic Carbon	-	-	72.5–1718 g/m^3	174–1850 g/m^3	-	-	-	195–651 g/m^3
Total Suspended Solids	4350 g/m^3	220–6400 g/m^3	0.390–9938 g/m^3	1068–6204 g/m^3	3696 g/m^3	58200 g/m^3	1121–1383 g/m^3	378–5462 g/m^3
FGO*	47.0 g/m^3	-	-	-	-	-	-	-
Total Nitrogen	-	50.0–840 g/m^3	60.0–339 g/m^3	-	-	-	327–525 g/m^3	163–564 g/m^3
Total Phosphorus	720 g/m^3	15.0–200 g/m^3	25.7–75.9 g/m^3		555 g/m^3	-	16–24 g/m^3	-
Sulphate	-	-	-	-	-	970 g/m^3	265–381 g/m^3	-
Nickel	-	-	-	4.02–8.61 g/m^3	<DL	-	-	-
Lead	-	-	-	-	<DL	-	-	-
Zinc	-	-	-	-	0.672 g/m^3	-	-	-
Copper	-	-	-	-	0.404 g/m^3	-	-	0.003–0.573 g/m^3
Cadmium	-	-	-	-	<DL	-	-	0.00002–0.034 g/m^3

* DL = Detection Limit

Table 3
Set of Impact Categories analysed in this study in alphabetical order.

Impact category	Unit
Acidification	mol H^+ eq
Climate change	kg CO_2 eq
Climate change - Fossil	kg CO_2 eq
Ecotoxicity, freshwater	CTUe
Eutrophication, freshwater	kg P eq
Eutrophication, marine	kg N eq
Eutrophication, terrestrial	mol N eq
Human toxicity, cancer	CTUh
Human toxicity, non-cancer	CTUh
Ionising radiation	kBq U-235 eq
Land use	Pt
Ozone depletion	kg CFC11 eq
Particulate matter	disease inc.
Photochemical ozone formation	kg NMVOC eq
Resource use, fossils	MJ
Resource use, minerals and metals	kg Sb eq
Water use	m^3 depriv.

accounted only in CML (Heijungs et al., 1992) and MEEuP impact assessment method, out of which only CML is available in SimaPro.

In terms of suspended solids from the poultry house wastewater, these are assumed to be bone debris of the carcasses and are modelled as calcium carbonate. Fat, grease and oil in wastewater are assumed to be poultry fat. Poultry fat typically contains a glycerol backbone with primary fatty acids, such as oleic acid (40.9 wt%), palmitic acid (20.9 wt %), and linoleic acid (20.5 wt%). Due to the lack of data in the ecoinvent database, only glycerol and oleic acid are modelled according to the weight ratio and the remaining fatty acids are modelled as generic fatty acids, C9–13-neo- | $C_{12}H_{24}O_2$ (Pubchem - Neododecanoic Acid Datasheet, 2023).

The sulphate content of the wastewater is modelled as sodium sulphate to represent the disassociated form in water, which provides sodium ions and sulphate ions. Sulphate ion is the only active ingredient. Since sodium ions are abundant in water, the environmental impact of sodium ion generation from sodium sulphate is assumed negligible.

The environmental impact of the transportation of water and sludge is assumed negligible compared to the operation of the wastewater treatment. Finally, the fate of sludge is assumed to be digested and incinerated for scenario 2 and only incinerated in scenario 3 as the organics in the sludge would have been digested by the additional step of membrane bioreactor in the treatment system.

3. Results

Section 3 presents the outputs of the process models using the PSM suite, which have been used to populate the Life Cycle Inventory (Section 3.1), and the results of the Life Cycle Impact Assessment, using the SimaPro software and the ecoinvent database (Section 3.2).

3.1. Life cycle inventory

Tables 4 and 5 illustrate the Life Cycle Inventory of the slaughterhouse wastewater for the three alternative scenarios, split between

Table 4
Life Cycle Inventory – Input with the functional unit as 1 m^3 of wastewater prior to entering the wastewater treatment system.

Resource	Scenario 1	Scenario 2	Scenario 3
Ferric (III) Chloride	-	462 g/m^3	462 g/m^3
Sodium Hydroxide	-	270 g/m^3	277 g/m^3
Flocculant	-	5.05 g/m^3	5.05 g/m^3
Hydrogen peroxide	-	-	50.0 g/m^3
Electricity (for coagulation)	-	0.276 kWh/m^3	0.276 kWh/m^3
Electricity (for DAF)	-	0.170 kWh/m^3	0.170 kWh/m^3
Electricity (for MBR)	-		2.95 kWh/m^3
Electricity (for AOP)	-		0.420 kWh/m^3

Table 5
Life Cycle Inventory – Output with the functional unit as 1 m^3 of wastewater prior to entering the wastewater treatment system.

Resource	Scenario 1 *	Scenario 2	Scenario 3
Alkalinity	85.0 g/m^3	54.2 g/m^3	57.1 g/m^3
pH	7.10	7.51	7.62
Chemical Oxygen Demand	1288 g/m^3	146 g/m^3	0.010 g/m^3
Biological Oxygen Demand	525 g/m^3	363 g/m^3	24.3 g/m^3
Total Organic Carbon	1570 g/m^3	160 g/m^3	0.160 g/m^3
Total Suspended Solids	686 g/m^3	103 g/m^3	1.03 g/m^3
FGO	183 g/m^3	4.80 g/m^3	4.80 g/m^3
Total Nitrogen	215 g/m^3	215 g/m^3	157 g/m^3
Total Phosphorus	33.5 g/m^3	33.5 g/m^3	0.000 g/m^3
Sulphate	622 g/m^3	622 g/m^3	617 g/m^3
Nickel	3.28 g/m^3	3.28 g/m^3	3.28 g/m^3
Lead	1.36 g/m^3	1.36 g/m^3	0.0300 g/m^3
Zinc	1.88 g/m^3	1.88 g/m^3	0.430 g/m^3
Copper	10.6 g/m^3	10.6 g/m^3	0.530 g/m^3
Cadmium	0.750 g/m^3	0.740 g/m^3	0.240 g/m^3
Sludge	-	0.510 m^3_{sludge}/h	1.37 m^3_{sludge}/h
Sludge (normalised per functional unit)	-	0.0124 m^3_{sludge}/h/m^3	0.0333 m^3_{sludge}/h/m^3
Wastewater	41.1 m^3/h	40.6 m^3/h	39.3 m^3/h

*Indicates experimental data, provided by an industrial unit

inputs (i.e. chemicals, energy) and outputs (i.e. emissions to water and byproducts). The Scenario 1 values in Table 5 correspond to the composition of the raw slaughterhouse wastewater.

For Scenario 2, the coagulation-flocculation process achieved 52% reduction in COD, which is similar to previously reported results (Amuda and Alade, 2006). In terms of total suspended solids, their concentration at the outlet of the dissolved air flotation tank was reduced by about 76% in comparison to the inlet, which is in accordance with the research of (Qamar et al., 2022), who stated that average COD removal efficiency was 71.13%. The wastewater treatment by dissolved air flotation enhanced the removal efficiency of COD, as reported also by (Del Nery et al., 2016). Overall, COD was removed by 88.6%, which is in agreement with the results obtained by (Tetteh and Rathilal, 2020).

For Scenario 3, the COD removal efficiency was estimated to be 99.9% following the wastewater treatment with the MBR and AOP (UV/H_2O_2). The result agrees with (Moser et al., 2018), where 97.5% COD removal efficiency was achieved with an initial concentration of 440 mg/L. It is worth mentioning that the simulation also confirmed that the membrane is capable of removing heavy metals. The removal efficiency was found to be 77%, 95%, 67%, and 98% for zinc, copper, cadmium and lead, respectively. Similar values were presented by (Tortora et al., 2016; Barakat and Schmidt, 2010; Rafique et al., 2015; Ferella et al., 2007), which were equal to 79%, 98%, 68%, and 99%. Regarding the advanced oxidation process using UV/H_2O_2, organic matter removal was achieved, and the pH was slightly influenced. The removal efficiency is confirmed by the research of (Bustillo-Lecompte et al., 2014).

3.2. Impact assessment

For Scenario 1, the normalised and weighted impact assessment and the breakdown of the environmental impact per flow (resource used or emission) are presented in Fig. 4. The environmental impacts estimated are solely the result of the quality of untreated wastewater. Freshwater eutrophication is the category with the highest impact (82.7%) amongst all normalised and weighted impacts studied, mainly due to nutrients, such as (ortho)phosphate, in wastewater (88.79%- 0.103 kg P eq), followed by waterborne emissions, such as COD (8.06%- 0.0935 kg P eq) and BOD (3.28%- 0.0038 kg P eq).

Freshwater ecotoxicity has the second highest impact (15.0%), mostly due to the presence of heavy metals in the effluent, in which copper has the highest share, contributing to 65.6% of the freshwater ecotoxicity impact category in Scenario 1. The remaining relevant impact categories for Scenario 1 (cancerous and non-cancerous human toxicity and marine eutrophication) have relatively low impact.

Fig. 5 illustrates the environmental impact assessment of Scenario 2, with the addition of primary treatment, namely coagulation, flocculation and DAF. The main share of the impact is due to the contaminants still present in the effluent stream compared to the impact of the treatment processes. Eutrophication of freshwater is still the category with the highest impact, 99.72% of which is due to the effluent, with minimal contribution from the rest of the processes and inputs. In agreement with Scenario 1, the second highest impact category is the freshwater ecotoxicity, whereby 96.02% of the impact is due to the effluent.

Fig. 5 also highlights the impact breakdown of each resource/process. The water treatment technologies applied in Scenario 2 have led to a variety of impacts of different magnitudes. Amongst all the impacts categories, the addition of the primary treatment results in the highest impact [0.019 milliEcopoints - mPt] in climate change. The lifecycle of the production of the flocculant has contributed 39.50% of the total impact of climate change, followed by the energy requirement (23.62%) for processing and incinerating the digested sludge (17.68%). The other significant impact categories are resource use (fossil fuels), freshwater ecotoxicity and marine eutrophication at 0.013, 0.012 and 0.011 mPt,

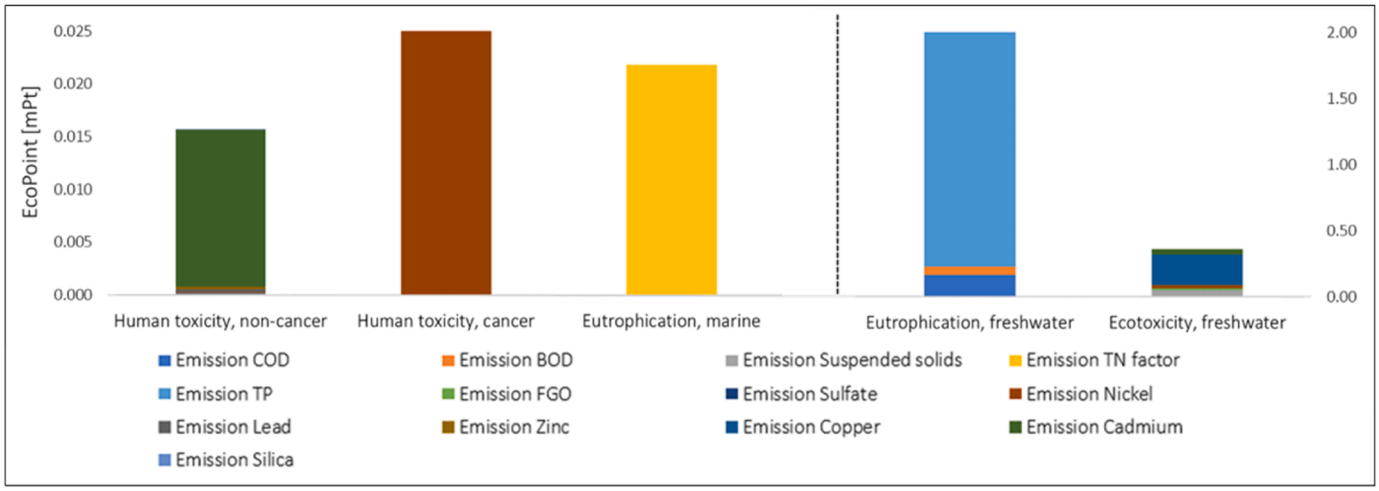

Fig. 4. Scenario 1 – Environmental Impact Assessment.

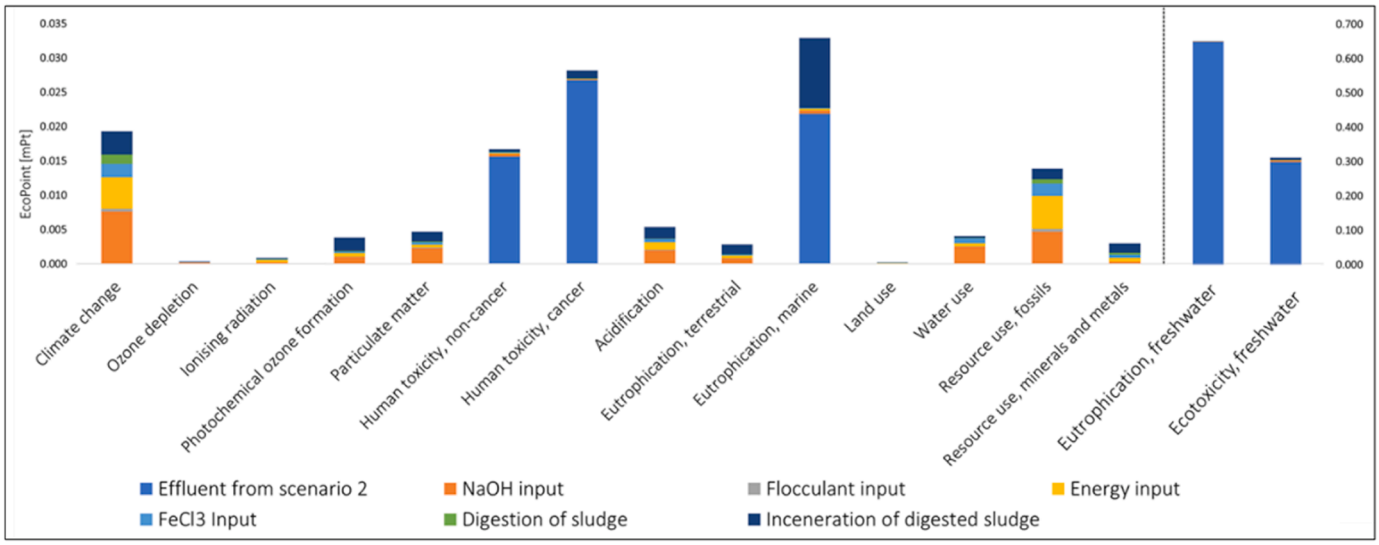

Fig. 5. Scenario 2 - Environmental Impact Assessment.

respectively.

Fig. 6 shows the normalised and weighted impact category of Scenario 3. In Scenario 3 the impact caused by the quality of the effluent and the treatment processes are on a comparable magnitude (contrary to Scenario 2 - Fig. 5). The three major sources of environmental impact for scenario 3 in descending order are the incineration of digested sludge, the quality of final effluent and the energy requirement for the MBR. The incineration of digested sludge has a higher impact due to more sludge

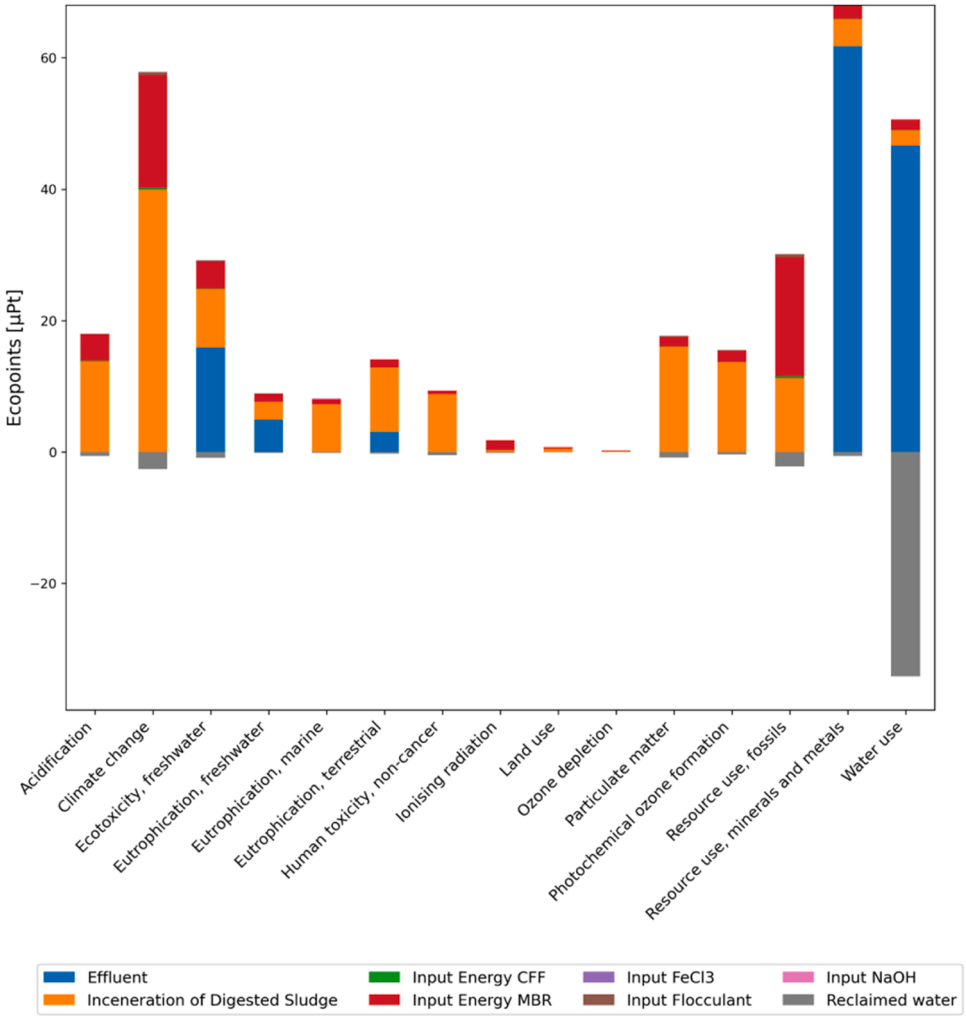

Fig. 6. Scenario 3 – Environmental Impact Assessment.

being produced per functional unit, thus, the environmental burden of the process also increases. In Scenario 3, freshwater ecotoxicity and climate change are the two categories with the highest impact, at 59.06 µPt and 55.24 µPt respectively. The tertiary treatment process (Scenario 3) has caused a significant reduction in the environmental impacts within the scope of the study. The negative signs for the impact categories show that the implementation of water reuse (30% in this case) in the slaughterhouse operation has resulted in a positive impact of 43.95 µPt on the environment. The reuse of the effluent after the tertiary treatment has multiple benefits since incorporating treated effluent back into the system not only reduces the water consumption for the slaughterhouse's daily operation but also offsets the environmental impact caused by the production process of an equal amount of tap water.

3.2.1. Scenario comparison

The baseline scenario (Scenario 1), which includes direct untreated discharge to a receiving water body without any onsite treatment, has the greatest environmental impact potential compared to the other two scenarios (Fig. 7), mostly due to the quality of contaminated effluents. The addition of CFF, DAF, MBR and AOP onsite treatment has resulted in the addition of the environmental impact categories of acidification, climate change, terrestrial eutrophication, ionising radiation, land use, ozone depletion, particulate matter, photochemical ozone formation, resource use (fossils), resource use (minerals and metals) and water use, due to the material and energy consumption for their operation. However, more significant environmental benefits were also achieved due to the superior effluent quality and the potential water reuse. For instance, the decrease in the freshwater eutrophication impact category is especially significant with increased treatment intensity (82.72% for Scenario 1 vs 53.94% for Scenario 2% and 2.71% for Scenario 3) relative to the total environmental impact of individual scenarios.

Freshwater ecotoxicity is the second most impacted category in all the scenarios at 14.66%, 27.52% and 23.12% respectively for each scenario. Overall, incorporating an onsite treatment system has resulted in a reduction of environmental impact, in Scenario 2 the total impact has reduced by 46% relative to the baseline scenario and a reduction of 90% in Scenario 3.

Accordingly, the best scenario for the slaughterhouse wastewater treatment is Scenario 3 with an overall footprint of 0.255 mPt, compared to 2.45 mPt and 1.31 mPt of the first and the second scenario, respectively.

4. Discussion and conclusions

In our work, the PSM Suite was used to model and simulate the production chain of a slaughterhouse, creating three alternative configurations. Based on the wastewater composition and the implementation of structured mathematical models, the quality of water at the outlet of each system is predicted. In addition, energy requirements and chemicals consumption are calculated, opening the way for a concrete environmental impact assessment.

Overall, this analysis highlights the importance of carefully considering the environmental impact of wastewater treatment methods. By using a comprehensive analysis that includes multiple impact categories, it is possible to identify the most environmentally friendly approach for a given scenario.

4.1. Main findings

Three different scenarios for the slaughterhouse wastewater treatment process were evaluated based on their environmental performance using Life Cycle Assessment. The method selected was the Environmental Footprint 3.0 with a functional unit of 1 m^3 wastewater influent, focusing only on the operational aspects of the system. The LCA showed that the quality of effluent stream has a higher influence on its environmental impact compared to the operation of the wastewater treatment processes (i.e. the additional energy and material required to purify the water) and the management of the produced solid waste.

The results from the analysis indicate that there is no clear "best" scenario for all impact categories. Instead, the most appropriate scenario will depend on the specific environmental priorities and the wastewater treatment system in question. For example, if the priority were to minimise eutrophication impacts, then Scenario 3 would be the most suitable, while if the focus were on reducing human toxicity (cancer) impacts, then Scenario 2 would be preferable.

Nevertheless, the implementation of MBR (tertiary treatment) seems to be very beneficial overall for the environmental impact. Although it has caused an increase in certain impact categories, these additional impacts have a relatively small influence on the environment, when the impacts are normalised. Scenario 3 is also characterised by a negative score for a few impacts, including water use, which indicates a positive environmental performance, due to the implemented water reuse. Therefore, Scenario 3, which was the most complex by involving the greater number of technologies, has the lowest impact between all three scenarios, due to the significant reduction of the contaminant

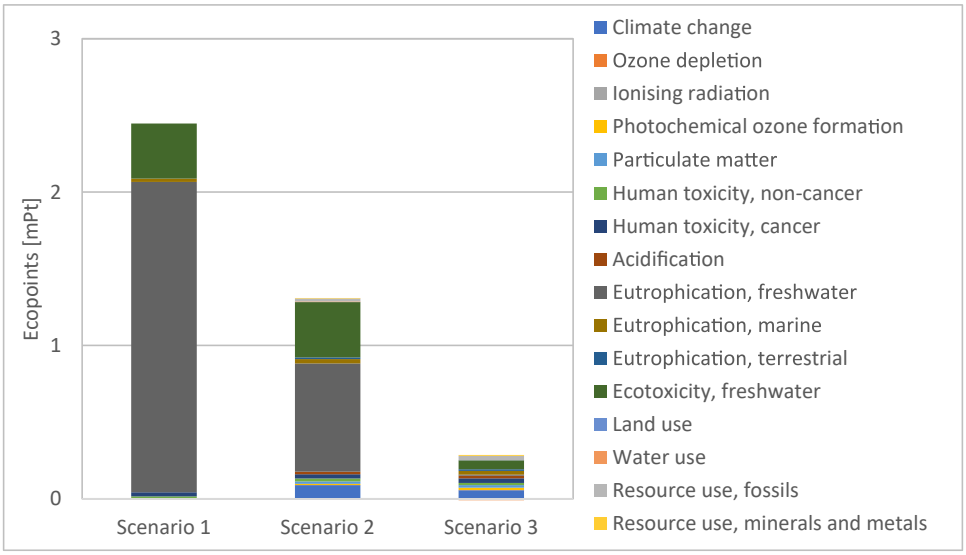

Fig. 7. Impact assessment comparison of 1 m^3 'Scenario 1', 1 m^3 'Scenario 2' and 1 m^3 'Scenario 3' using EF 3.0 Method (weighted and normalised).

concentration in the wastewater stream and the partial water reuse achieved.

4.2. Limitations of the study

In this study, only three different scenarios are modelled and assessed. We have not included other common practices, such as the pre-treatment of slaughterhouse wastewater and co-treatment with municipal wastewater before being discharged to surface water. On that note, it has to be pointed out that one major assumption, on which the analysis was based on, is that only 30% of the treated water will be reused to the slaughterhouse, thus reducing both the potential water depletion and the need for the energy and chemical intensive process of water treatment before being used. The selected percentage does not cover the entire water requirements of the slaughterhouse, since the quality of the treated wastewater is only appropriate for a range of the slaughterhouse's operation. Thus, greater benefits can be potentially achieved through further treatment of the wastewater and increase of the water reuse share. On the other hand, additional consumers for the treated wastewater could be sought in the neighbouring industrial, agricultural or municipal stakeholders, towards the formulation of industrial symbiosis schemes. Although this will not further reduce the slaughterhouse's footprint, it will have positive impacts to the overall environmental impact from a holistic systemic perspective. However, as demonstrated in this study, every additional step will result in different impacts on the environment, either due to further resource consumption for wastewater treatment or due to water transportation. Thus, further analysis is required for each new scenario before making a decision.

The assumptions of the process modelling part, in terms of the operating conditions, consist another limitation of the present work, due to the lack of pilot-scale experimental data. Such data would contribute to the validation of the developed model. Furthermore, the accuracy of our analysis may be significantly improved if the literature data, which were used for the chemicals consumption and power requirements, would be substituted for real-time data.

Finally, for the LCA inventory of the quality of effluent, only emissions to water are considered, whereas airborne and landborne transmission of the pollutants have been ignored in this study. One of the prevailing limitations inherent in LCA studies is the absence of uniformity in both the methodology and the methodologies employed in data collection. While certain investigations may rely on data sourced from databases, others may lean on data specific to a given site acquired through direct measurements (Ferella et al., 2007; Bustillo-Lecompte et al., 2014). In this study, a holistic approach is adopted, coupling on-site measurements with experimental study and modelling techniques. Notably, different studies may adopt different functional units, different system boundaries and allocation methods, appraise diverse impact categories, and utilise varying sources of data which can affect the results and the comparability of the studies. Whilst this LCA study contributed to understanding the source of environmental impact from individual pollutants, it should be emphasised that the analysis does not distribute the consequences linked with co-products, such as the energy co-generation facilitated through biogas yielded from the incineration of sludge. In addition, another limitation of this study is that it does not include economic analysis. Future research should explore the integration of economic analysis into LCA to provide a more comprehensive and well-informed assessment of the environmental and economic performance of alternative process design decision scenarios. Consequently, this study presents an opportunity for subsequent investigations to introduce a system expansion by retro integrating the assessment of impacts associated with such co-products.

Declaration of Competing Interest

The authors declare that they have no known competing financial interests or personal relationships that could have appeared to influence the work reported in this paper.

Acknowledgments

The Technology Modelling presented in the paper arises from "AquaSPICE - Advancing Sustainability of Process Industries through Digital and Circular Water Use Innovations", a collaborative research project that has received funding from the European Union's Horizon 2020 research and innovation programme under Grant Agreement No 958396.

Appendix

Table A1
Process variables of the MBR model.

Process variable	Symbol	Unit
Readily biodegradable soluble substrate	S_S	mg COD/L
Slowly biodegradable particulate substrate	X_S	mg COD/L
Active heterotrophic particulate biomass	$X_{B,H}$	mg COD/L
Active autotrophic particulate biomass	$X_{B,A}$	mg COD/L
Soluble oxygen	S_O	mg/L
Soluble nitrate and nitrite nitrogen	S_{NO}	mg N/L
Soluble ammonium nitrogen	S_{NH}	mg N/L
Soluble biodegradable organic nitrogen	S_{ND}	mg N/L
Particulate biodegradable organic nitrogen	X_{ND}	mg N/L
Inert soluble organic matter	S_I	mg COD/L
Particulate inert organic matter	X_I	mg COD/L
Particulate products derived from the biomass decay	X_P	mg COD/L

Table A2
Kinetic and stoichiometric parameters for the MBR model.

Parameter	Symbol	Unit	Reference
Yield for autotrophic biomass	Y_A	0.24 g COD/g N	(Henze et al., 2002; Lahdhiri et al., 2020)
Yield for heterotrophic biomass	Y_H	0.67 g COD/g N	(Henze et al., 2002; Lahdhiri et al., 2020)
Decay coefficient for autotrophic biomass	b_A	0.05 1/d	(Nelson et al., 2019)
Decay coefficient for heterotrophic biomass	b_H	0.62 1/d	(Henze et al., 2002; Lahdhiri et al., 2020)
Fraction of biomass resulting in particulate products	f_P	0.08	(Henze et al., 2002; Lahdhiri et al., 2020)
Mass of nitrogen per COD in biomass	i_{XB}	0.086 g N/g COD	(Henze et al., 2002; Lahdhiri et al., 2020)

(continued on next page)

Table A2 (*continued*)

Parameter	Symbol	Unit	Reference
Mass of Nitrogen per COD in products derived from biomass	i_{XP}	0.06 g N/g COD	(Henze et al., 2002; Lahdhiri et al., 2020)
Oxygen half-saturation coefficient for heterotrophic biomass	$K_{O,H}$	0.20 mg O_2/L	(Henze et al., 2002; Wu et al., 2016)
Oxygen half-saturation coefficient for denitrifying heterotrophic biomass	K_{NO}	0.50 mg N/L	(Henze et al., 2002)
Oxygen half-saturation coefficient for autotrophic biomass	$K_{O,A}$	0.40 mg O_2/L	(Henze et al., 2002)
Maximum specific growth rate for autotrophic biomass	$\mu_{max,A}$	0.80 1/d	(Henze et al., 2002; Lahdhiri et al., 2020)
Maximum specific growth rate for heterotrophic biomass	$\mu_{max,H}$	6.00 1/d	(Lindamulla et al., 2021; Henze et al., 2002; Lahdhiri et al., 2020)
Ammonia half-saturation coefficient for autotrophic biomass	K_{NH}	1.00 mg N/L	(Lindamulla et al., 2021; Henze et al., 2002; Wu et al., 2016)
Correction factor for maximum specific growth rate for heterotrophic biomass under anoxic conditions	η_g	0.80	(Henze et al., 2002)
Correction factor for hydrolysis under anoxic conditions	η_h	0.40	(Henze et al., 2002)
Half-saturation coefficient for heterotrophic biomass	K_S	20.00 mg COD/L	(Deowan et al., 2019; Henze et al., 2002; Lahdhiri et al., 2020)
Half-saturation coefficient for hydrolysis of slowly biodegradable particulate substrate	K_X	0.03 g COD/g COD	(Henze et al., 2002; Lahdhiri et al., 2020)
Hydrolysis coefficient	k_h	3.00 g COD/g COD/d	(Henze et al., 2002; Lahdhiri et al., 2020)
Oxygen transfer coefficient	K_{LA}	108 d^{-1}	(Nelson et al., 2019)
Maximum concentration of soluble oxygen	$S_{O,max}$	10.00 mg O_2/L	(Nelson et al., 2019)
Ammonification rate	k_a	0.08	(Henze et al., 2002)
Recycle ratio	R	0.40	(Nelson et al., 2019)
Wasted fraction	w_1	0.10	(Nelson et al., 2019)
Concentrating factor for particulates in the membrane	b	calculated	N/A
Internal recycle stream from aeration to anoxic tank	r_{int}	1.61	(Judd et al., 2011)
Membrane recirculation ratio	r_{mr}	4	(Judd et al., 2011)

Table A3
The reactions involved in the AOP model and the relevant reaction rate constants.

Reaction	Rate constant	Reference
$H_2O_2 \rightarrow 2\ HO^{\bullet}$	0.5 mol/Ein	(Rubio-Clemente et al., 2017; Ameta and Ameta, 2018)
$HO^{\bullet} + HO_2^{\bullet} \rightarrow O_2 + H_2O$	$6.6 \bullet 10^9$ 1/mol/L/s	(Wols et al., 2015; Song et al., 2008; Hu et al., 2019)
$H_2O_2 + HO^{\bullet} \rightarrow HO_2^{\bullet} + H_2O$	$2.7 \bullet 10^7$ 1/mol/L/s	(Ameta and Ameta, 2018; Song et al., 2008)
$HO_2^{\bullet} + H_2O_2 \rightarrow HO^{\bullet} + H_2O + O_2$	3.0 1/mol/L/s	(Ameta and Ameta, 2018; Crittenden et al., 1999; Yang et al., 2016)
$HO_2^{\bullet} + O_2^{\bullet-} \rightarrow HO_2^- + O_2$	$9.7 \bullet 10^7$ 1/mol/L/s	(Wols et al., 2015; Song et al., 2008)
$HO^{\bullet} + O_2^{\bullet-} \rightarrow OH^- + O_2$	$8.0 \bullet 10^9$ 1/mol/L/s	(Song et al., 2008)
$H_2O_2 + O_2^{\bullet-} \rightarrow HO^{\bullet} + O_2 + OH^-$	0.13 1/mol/L/s	(Wols et al., 2015; Song et al., 2008)
$HO^{\bullet} + HO_2^- \rightarrow HO_2^{\bullet} + OH^-$	$7.5 \bullet 10^9$ 1/mol/L/s	(Ameta and Ameta, 2018; Song et al., 2008)
$H_2O_2 \rightarrow HO_2^- + H^+$	0.025 1/mol/L/s	(Wols et al., 2015)
$HO_2^- + H^+ \rightarrow H_2O_2$	$1.0 \bullet 10^{10}$ 1/mol/L/s	(Wols et al., 2015)]
$HO_2^{\bullet} \rightarrow O_2^{\bullet-} + H^+$	$1.58 \bullet 10^5$ 1/mol/L/s	(Wols et al., 2015)
$O_2^{\bullet-} + H^+ \rightarrow HO_2^{\bullet}$	$1.0 \bullet 10^{10}$ 1/mol/L/s	(Wols et al., 2015)
$HO^{\bullet} + HO^{\bullet} \rightarrow H_2O_2$	$5.5 \bullet 10^9$ 1/mol/L/s	(Wols et al., 2015; Hu et al., 2019)
$HO_2^{\bullet} + HO_2^{\bullet} \rightarrow H_2O_2 + O_2$	$8.6 \bullet 10^5$ 1/mol/L/s	(Song et al., 2008)
$HO^{\bullet} + CO_3^{2-} \rightarrow CO_3^{\bullet-} + OH^-$	$3.9 \bullet 10^8$ 1/mol/L/s	(Song et al., 2008)
$HO^{\bullet} + HCO_3^- \rightarrow CO_3^{\bullet-} + H_2O$	$8.5 \bullet 10^6$ 1/mol/L/s	(Song et al., 2008)
$HO^{\bullet} + CO_3^{\bullet-} \rightarrow CO_3^{2-} + OH^-$	$3.0 \bullet 10^9$ 1/mol/L/s	(Song et al., 2008)
$H_2O_2 + CO_3^{\bullet-} \rightarrow HCO_3^- + HO_2^{\bullet}$	$4.3 \bullet 10^5$ 1/mol/L/s	(Crittenden et al., 1999)
$CO_3^{\bullet-} + HO_2^- \rightarrow CO_3^{2-} + HO_2^{\bullet}$	$3.0 \bullet 10^7$ 1/mol/L/s	(Song et al., 2008)
$CO_3^{\bullet-} + O_2^{\bullet-} \rightarrow CO_3^{2-} + O_2$	$6.0 \bullet 10^8$ 1/mol/L/s	(Crittenden et al., 1999)
$CO_3^{\bullet-} + CO_3^{\bullet-} \rightarrow 2\ CO_3^{2-}$	$3.0 \bullet 10^7$ 1/mol/L/s	(Wols et al., 2015)
$HCO_3^- \rightarrow CO_3^{2-} + H^+$	$1.0 \bullet 10^{10}$ 1/mol/L/s	(Wols et al., 2015)
$CO_3^{2-} + H^+ \rightarrow HCO_3^-$	0.45 1/s	(Wols et al., 2015)
$H_2CO_3 \rightarrow HCO_3^- + H^+$	$1.0 \bullet 10^{10}$ 1/mol/L/s	(Wols et al., 2015)
$HCO_3^- + H^+ \rightarrow H_2CO_3$	$4.5 \bullet 10^3$ 1/mol/L/s	(Wols et al., 2015)
$HO^{\bullet} + H_2PO_4^- \rightarrow HPO_4^{\bullet-} + H_2O$	$2.0 \bullet 10^4$ 1/mol/L/s	(Yang et al., 2016)
$HO^{\bullet} + HPO_4^{2-} \rightarrow HPO_4^{\bullet-} + OH^-$	$1.5 \bullet 10^5$ 1/mol/L/s	(Yang et al., 2016)
$H_2O_2 + HPO_4^{\bullet-} \rightarrow H_2PO_4^- + HO_2^{\bullet}$	$2.7 \bullet 10^7$ 1/mol/L/s	(Yang et al., 2016)
$PO_4^{3-} + H^+ \rightarrow HPO_4^{2-}$	$5.0 \bullet 10^{10}$ 1/mol/L/s	(Yang et al., 2016)
$HPO_4^{2-} \rightarrow PO_4^{3-} + H^+$	$2.5 \bullet 10^{-2}$ 1/mol/L/s	(Yang et al., 2016)
$HPO_4^{2-} + H^+ \rightarrow H_2PO_4^-$	$5.0 \bullet 10^{10}$ 1/mol/L/s	(Yang et al., 2016)
$H_2PO_4^- \rightarrow HPO_4^{2-} + H^+$	$3.2 \bullet 10^3$ 1/mol/L/s	(Yang et al., 2016)
$H_2PO_4^- + H^+ \rightarrow H_3PO_4$	$5.0 \bullet 10^{10}$ 1/mol/L/s	(Yang et al., 2016)
$H_3PO_4 \rightarrow H_2PO_4^- + H^+$	$3.97 \bullet 10^8$ 1/s	(Yang et al., 2016)
$HO^{\bullet} + HSO_4^- \rightarrow SO_4^{\bullet-} + H_2O$	$3.5 \bullet 10^5$ 1/mol/L/s	(Rubio-Clemente et al., 2017)
$H_2O_2 + SO_4^{\bullet-} \rightarrow SO_4^{2-} + HO_2^{\bullet} + H^+$	$1.2 \bullet 10^7$ 1/mol/L/s	(Rubio-Clemente et al., 2017)
$HO_2^{\bullet} + SO_4^{\bullet-} \rightarrow SO_4^{2-} + O_2 + H^+$	$3.5 \bullet 10^9$ 1/mol/L/s	(Rubio-Clemente et al., 2017)
$HSO_4^- \rightarrow SO_4^{2-} + H^+$	$1.0 \bullet 10^{10}$ 1/mol/L/s	(Rubio-Clemente et al., 2017)
$SO_4^{2-} + H^+ \rightarrow HSO_4^-$	$45 \bullet 10^{10}$ 1/mol/L/s	(Rubio-Clemente et al., 2017)
$ONOOH \rightarrow ONOO^- + H^+$	$1.0 \bullet 10^{10}$ 1/mol/L/s	(Wols et al., 2015)
$ONOO^- + H^+ \rightarrow ONOOH$	$2.5 \bullet 10^3$ 1/mol/L/s	(Wols et al., 2015)
$ONOO^- \rightarrow NO^{\bullet} + O_2^{\bullet-}$	0.017 1/s	(Wols et al., 2015)
$NO_3^- \rightarrow ONOO^-$	0.1 mol/Ein	(Mark et al., 1996)
$NO_3^- \rightarrow NO_2^{\bullet} + O^{\bullet-}$	0.09 mol/Ein	(Mark et al., 1996)
$NO^{\bullet} + O_2^{\bullet-} \rightarrow ONOO^-$	$5.0 \bullet 10^9$ 1/mol/L/s	(Wols et al., 2015)

(*continued on next page*)

Table A3 (*continued*)

Reaction	Rate constant	Reference
$HO^{\bullet} + ONOO^{-} \rightarrow NO_2^{-} + O_2^{\bullet-} + H^{+}$	$4.8 \bullet 10^{9}$ 1/mol/L/s	(Wols et al., 2015)
$HO^{\bullet} + NO_2^{-} \rightarrow NO_2^{\bullet} + OH^{-}$	$1.0 \bullet 10^{10}$ 1/mol/L/s	(Wols et al., 2015)
$O_2^{\bullet-} + NO_2^{\bullet} \rightarrow NO_2^{-} + O_2$	$4.8 \bullet 10^{9}$ 1/mol/L/s	(Wols et al., 2015)
$HO_2^{\bullet} + NO_2^{\bullet} \rightarrow NO_2^{-} + O_2 + H^{+}$	$1.8 \bullet 10^{9}$ 1/mol/L/s	(Wols et al., 2015)
$NO^{\bullet} + NO_2^{\bullet} \rightarrow N_2O_3$	$1.1 \bullet 10^{9}$ 1/mol/L/s	(Wols et al., 2015)
$N_2O_3 \rightarrow NO^{\bullet} + NO_2^{\bullet}$	$8.4 \bullet 10^{4}$ 1/s	(Wols et al., 2015)
$NO_2^{\bullet} + NO_2^{\bullet} \rightarrow N_2O_4$	$4.5 \bullet 10^{8}$ 1/mol/L/s	(Wols et al., 2015)
$N_2O_4 \rightarrow NO_2^{\bullet} + NO_2^{\bullet}$	$0.69 \bullet 10^{4}$ 1/s	(Wols et al., 2015)
TOC →intermediates→CO_2 +H_2O	0.14 mol/Ein	(Song et al., 2008)
TOC+$HO^{\bullet}$→intermediates→ CO_2 + H_2O	$7.0 \bullet 10^{5}$ 1/mol/L/s	(Bustillo-Lecompte et al., 2016)

References

Ahmed, M., Mavukkandy, M.O., Giwa, A., Elektorowicz, M., Katsou, E., Khelifi, O., Naddeo, V., Hasan, S.W., 2022. Recent developments in hazardous pollutants removal from wastewater and water reuse within a circular economy. npj Clean. Water 5, 12. https://doi.org/10.1038/s41545-022-00154-5.

S.C. Ameta, R. Ameta, Advanced Oxidation Processes for Wastewater Treatment, Emerging Green Chemical Technology. 2018.

Amin, A., Al Bazedi, G., Abdel-Fatah, M.A., 2021. Experimental study and mathematical model of coagulation/sedimentation units for treatment of food processing wastewater. Ain Shams Eng. J. 12, 195–203. https://doi.org/10.1016/j.asej.2020.08.001.

Amuda, O.S., Alade, A., 2006. Coagulation/flocculation process in the treatment of abattoir wastewater. Desalination 196, 22–31. https://doi.org/10.1016/j.desal.2005.10.039.

Aziz, A., Basheer, F., Sengar, A., Irfanullah, Khan, S.U., Farooqi, I.H., 2019. Biological wastewater treatment (anaerobic-aerobic) technologies for safe discharge of treated slaughterhouse and meat processing wastewater. Sci. Total Environ. 686, 681–708. https://doi.org/10.1016/j.scitotenv.2019.05.295.

Barakat, M.A., Schmidt, E., 2010. Polymer-enhanced ultrafiltration process for heavy metals removal from industrial wastewater. Desalination 256, 90–93. https://doi.org/10.1016/j.desal.2010.02.008.

Baruth, E.E., 2005. Water treatment plant design. McGraw-Hill.

Behin, J., Bahrami, S., 2012. Modeling an industrial dissolved air flotation tank used for separating oil from wastewater. Chem. Eng. Process. Process. Intensif. 59, 1–8. https://doi.org/10.1016/j.cep.2012.05.004.

Brown, V., Jackson, D.W., Khalifé, M., 2010. Melbourne metropolitan sewerage strategy: a portfolio of decentralised and on-site concept designs. Water Sci. Technol. 62, 510–517. https://doi.org/10.2166/wst.2010.296.

Bustillo-Lecompte, C., Mehrvar, M., 2017. Slaughterhouse wastewater: treatment, management and resource recovery. Phys. -Chem. Wastewater Treat. Resour. Recover. https://doi.org/10.5772/65499.

Bustillo-Lecompte, C.F., Mehrvar, M., 2015. Slaughterhouse wastewater characteristics, treatment, and management in the meat processing industry: a review on trends and advances. J. Environ. Manag. 161, 287–302. https://doi.org/10.1016/j.jenvman.2015.07.008.

Bustillo-Lecompte, C.F., Ghafoori, S., Mehrvar, M., 2016. Photochemical degradation of an actual slaughterhouse wastewater by continuous UV/H_2O_2 photoreactor with recycle. J. Environ. Chem. Eng. 4, 719–732. https://doi.org/10.1016/j.jece.2015.12.009.

Bustillo-Lecompte, D.F., Mehrvar, M., Quiñones-Bolaños, E., 2014. Cost-effectiveness analysis of TOC removal from slaughterhouse wastewater using combined anaerobic-aerobic and UV/H_2O_2 processes. J. Environ. Manag. 134, 145–152. https://doi.org/10.1016/j.jenvman.2013.12.035.

Çetinkaya, A., Bilgili, L., 2022. Treatment of slaughterhouse industry wastewater with ultrafiltration membrane and evaluation with life cycle analysis. Environ. Res. Tech. 5 (3), 197–201. https://doi.org/10.35208/ert.1102829.

Chung, G., Lansey, K., Blowers, P., Brooks, P., Ela, W., Stewart, S., Wilson, P., 2008. A general water supply planning model: evaluation of decentralized treatment. Environ. Model. Softw. 23, 893–905. https://doi.org/10.1016/j.envsoft.2007.10.002.

Corominas, L., Byrne, D.M., Guest, J.S., Hospido, A., Roux, P., Shaw, A., Short, M.D., 2020. The application of life cycle assessment (LCA) to wastewater treatment: a best practice guide and critical review. Water Res 184, 116058. https://doi.org/10.1016/j.watres.2020.116058.

Crittenden, J.C., Hu, S., Hand, D.W., Green, S.A., 1999. A kinetic model for H_2O_2/UV process in a completely mixed batch reactor. Water Res. 33, 2315–2328 https://10.1016/S0043-1354(98)00448-5.

Davarnejad, R., Nasiri, S., 2017. Slaughterhouse wastewater treatment using an advanced oxidation process: optimization study. Environ. Pollut. 223, 1–10. https://doi.org/10.1016/j.envpol.2016.11.008.

Del Nery, V., de Nardi, I.R., Damianovic, M.H.R.Z., Pozzi, E., Amorim, A.K.B., Zaiat, M., 2007. Long-term operating performance of a poultry slaughterhouse wastewater treatment plant. Resour. Conserv. Recycl. 50, 102–114. https://doi.org/10.1016/j.resconrec.2006.06.001.

Del Nery, V., Damianovic, M.H.Z., Moura, R.B., Pozzi, E., Pires, E.C., Foresti, E., 2016. Poultry slaughterhouse wastewater treatment plant for high quality effluent. Water Sci. Technol. 73 (2), 309–316. https://doi.org/10.2166/wst.2015.494.

Deng, Y., Zhao, R., 2015. Advanced oxidation processes (AOPs) in wastewater treatment. Curr. Pollut. Rep. 1, 167–176. https://doi.org/10.1007/s40726-015-0015-z.

Deowan, S.A., Korejba, W., Hoinkis, J., Figoli, A., Drioli, E., Islam, R., Jamal, L., 2019. Design and testing of a pilot-scale submerged membrane bioreactor (MBR) for textile wastewater treatment. Appl. Water Sci. 9 https://doi.org/10.1007/s13201-019-0934-8.

Ding, A., Zhang, R., Ngo, H.H., He, X., Ma, J., Nan, J., Li, G., 2021. Life cycle assessment of sewage sludge treatment and disposal based on nutrient and energy recovery: a review. Sci. Total Environ. 769, 144451 https://doi.org/10.1016/j.scitotenv.2020.144451.

Edzwald, J.K., 2010. Dissolved air flotation and me. Water Res 44, 2077–2106. https://doi.org/10.1016/j.watres.2009.12.040.

Ehteshami, M., Maghsoodi, S., Yaghoobnia, E., 2015. Optimum turbidity removal by coagulation/flocculation methods from wastewaters of natural stone processing. Desalin. Water Treat. 57, 20749–20757. https://doi.org/10.1080/19443994.2015.1110725.

EU Commission, Environmental Footprints Methods, Available at: ⟨https://ec.europa.eu/environment/eussd/smgp/pdf/EF%20simple%20guide_v7_clen.pdf⟩ (Accessed 01 March 2023).

Ferella, F., Prisciandaro, M., De Michelis, I., Veglio, F., 2007. Removal of heavy metals by surfactant-enhanced ultrafiltration from wastewaters. Desalination 207, 125–133. https://doi.org/10.1016/j.desal.2006.07.007.

Gautam, R.K., Olubukola, A., More, N., Jegatheesan, V., Muthukumaran, S., Navaratna, D., 2023. Evaluation of long-term operational and treatment performance of a high-biomass submerged anaerobic membrane bioreactor treating abattoir wastewater. Chem. Eng. J. 463, 142145 https://doi.org/10.1016/j.cej.2023.142145.

Genné, I., Derden, A., 2008. A. Water and energy management in the slaughterhouse. Handb. Water Energy Manag. Food Process 805–815. https://doi.org/10.1533/9781845694678.6.805.

Gerbens-Leenes, P.W., Mekonnen, M.M., Hoekstra, A.Y., 2013. The water footprint of poultry, pork and beef: a comparative study in different countries and production systems. Water Resour. Ind. 1–2, 25–36. https://doi.org/10.1016/j.wri.2013.03.001.

Gkika, D.A., Mitropoulos, A.C., Lambropoulou, D.A., Kalavrouziotis, I.K., Kyzas, G.Z., 2022. Cosmetic wastewater treatment technologies: a review. Environ. Sci. Pollut. Res. 29, 75223–75247. https://doi.org/10.1007/s11356-022-23045-1.

Glaze, W.H., Lay, Y., Kang, J.W., 1995. Advanced oxidation processes. a kinetic model for the oxidation of 1,2-dibromo-3-chloropropane in water by the combination of hydrogen peroxide and UV radiation. Ind. Eng. Chem. Res. 34, 2314–2323. https://doi.org/10.1021/ie00046a013.

Grebel, J.E., Pignatello, J.J., Mitch, W.A., 2010. Effect of halide ions and carbonates on organic contaminant degradation by hydroxyl radical-based advanced oxidation processes in saline waters. Environ. Sci. Technol. 44, 6822–6828. https://doi.org/10.1021/es1010225.

Green, D.W., Southard, M.Z., 2019. Perry's Chemical Engineers' Handbook, nineth ed. Mc Graw Hill Education.

Gulhan, H., Dereli, R.K., Ersahin, M.E., Koyuncu, İ., 2022. Dynamic modeling of a full-scale membrane bioreactor performance for landfill leachate treatment. Bioprocess Biosyst. Eng. 45, 345–352. https://doi.org/10.1007/s00449-021-02664-x.

Gutu, L., Basitere, M., Harding, T., Ikumi, D., Njoya, M., Gaszynski, C., 2021. Multi-integrated systems for treatment of abattoir wastewater: a review. Water 13, 2462. https://doi.org/10.3390/w13182462.

F.I. Hai, K. Yamamoto, C.-H. Lee, Membrane Biological Reactors Theory, Modeling, Design, Management and Applications to Wastewater Reuse. IWA Publishing, 2014b.

Hai, F.I., Yamamoto, K., Lee, C.H., 2014a. Membrane biological reactors. Theory, Modeling, Design, Management and Applications to Wastewater Reuse. IWA Publishing.

Hassaan, M.A., El Nemr, A., El-Zahhar, A.A., Idris, A.M., Alghamdi, M.M., Sahlabji, T., Said, T.O., 2022. Degradation mechanism of Direct Red 23 dye by advanced oxidation processes: a comparative study. Toxin Rev. 41, 38–47. https://doi.org/10.1080/15569543.2020.1827431.

Heijungs, R., Guinée, J., Huppes, G., Lankreijer, R.M., Udo de Haes, H.A., Wegener Sleeswijk, A., Ansems, A.M.M., Eggels, P.G., van Duin, R., de Goede, H.P., 1992.

Environmental life cycle assessment of products. Guide and backgrounds. Cent. Environ. Sciense (CML). (part 1).
Henze, M., Gujer, W., Mino, T., van Loosdrecht, M., 2002. Activated sludge models ASM1, ASM2, ASM2d and ASM3. Sci. Tech. Rep. 9.
Ho, G., Martin, A., 2006. A. Centralised versus decentralised wastewater systems in an urban context: the sustainability dimension. 2nd IWA Lead. edge Sustain. Water-limited Environ. IWA Publ., pp. 80–89
Hu, C.-Y., Hou, Y.-Z., Lin, Y.-L., Deng, Y.-G., Hua, S.-J., Du, Y.-F., Chen, C.-W., Wu, C.-H., 2019. Kinetics and model development of iohexol degradation during UV/H_2O_2 and UV/$S_2O_8^{2-}$ oxidation. Chemosphere 229, 602–610. https://doi.org/10.1016/j.chemosphere.2019.05.012.
Ismail, L., Ferronato, C., Fine, L., Jaber, F., Chovelon, J.-M., 2018. Effect of water constituents on the degradation of sulfaclozine in the three systems: UV/TiO_2, UV/$K_2S_2O_8$, and UV/TiO_2/$K_2S_2O_8$. Environ. Sci. Pollut. Res. 25, 2651–2663. https://doi.org/10.1007/s11356-017-0629-3.
Jensen, P.D., Yap, S.D., Boyle-Gotla, A., Janoschka, J., Carney, C., Pidou, M., Batstone, D. J., 2015. Anaerobic membrane bioreactors enable high rate treatment of slaughterhouse wastewater. Biochem. Eng. J. 97, 132–141. https://doi.org/10.1016/j.bej.2015.02.009.
Johansson, K., Perzon, M., Fröling, M., Mossakowska, A., Svanström, M., 2008. Sewage sludge handling with phosphorus utilization - life cycle assessment of four alternatives. J. Clean. Prod. 16, 135–151. https://doi.org/10.1016/j.jclepro.2006.12.004.
JRC EU, Recommendations for Life Cycle ImpactAssessment in the European context, Available at ⟨https://eplca.jrc.ec.europa.eu/uploads/ILCD-Recommendation-of-methods-for-LCIA-def.pdf⟩ (Accessed 01 March 2023).
S. Judd, C. Judd, The M.B.R. Book. Principles and Applications of Membrane Bioreactors for Water and Wastewater Treatment, IWA Publising. 2011.
Jung, H.J., Lee, J.W., Choi, D.Y., Kim, S.J., Kwak, D.H., 2006. Flotation efficiency of activated sludge flocs using population balance model in dissolved air flotation. Korean J. Chem. Eng. 23, 271–278. https://doi.org/10.1007/BF02705726.
Kanafin, Y.N., Makhatova, A., Meiramkulova, K., Poulopoulos, S.G., 2022. Treatment of a poultry slaughterhouse wastewater using advanced oxidation processes. J. Water Process Eng. 47, 102694 https://doi.org/10.1016/j.jwpe.2022.102694.
Lahdhiri, A., Lesage, G., Hannachi, A., Heran, M., 2020. Steady-state methodology for activated sludge model 1 (ASM1) state variable calculation in MBR. Water 12, 1–13. https://doi.org/10.3390/w12113220.
Libralato, G., Volpi Ghirardini, A., Avezzù, F., 2012. To centralise or to decentralise: an overview of the most recent trends in wastewater treatment management. J. Environ. Manag. 94, 61–68. https://doi.org/10.1016/j.jenvman.2011.07.010.
Lindamulla, L.M.L.K.B., Jegatheesan, V., Jinadasa, K.B.S.N., Nanayakkara, K.G.N., Othman, M.Z., 2021. Integrated mathematical model to simulate the performance of a membrane bioreactor. Chemosphere 284, 131319. https://doi.org/10.1016/j.chemosphere.2021.131319.
Liu, X., Liu, Y., Lu, S., Wang, Z., Wang, Y., Zhang, G., Guo, X., Guo, W., Zhang, T., Xi, B., 2020. Degradation difference of ofloxacin and levofloxacin by UV/H_2O_2 and UV/PS (persulfate): efficiency, factors and mechanism. Chem. Eng. J. 385, 123987 https://doi.org/10.1016/j.cej.2019.123987.
Liu, Y., Kang, X., Li, X., Yuan, Y., 2015. Performance of aerobic granular sludge in a sequencing batch bioreactor for slaughterhouse wastewater treatment. Bioresour. Technol. 190, 487–491. https://doi.org/10.1016/j.biortech.2015.03.008.
Lombardi, L., Nocita, C., Bettazzi, E., Fibbi, D., Carnevale, E., 2017. Environmental comparison of alternative treatments for sewage sludge: An Italian case study. Waste Manag 69, 365–376. https://doi.org/10.1016/j.wasman.2017.08.040.
J. Lundqvist, C. de Fraiture, D.J. Molden, Saving Water: From Field to Fork: Curbing Losses and Wastage in the Food Chain. SIWI Policy Brief (2008).
Mack, J., Bolton, J.R., 1999. Photochemistry of nitrite and nitrate in aqueous solution: a review. J. Photochem. Photobiol. A Chem. 128, 1–13. https://doi.org/10.1016/S1010-6030(99)00155-0.
Madeira, L., Ribau Teixeira, M., Almeida, A., Santos, T., Carvalho, F., 2023. Reuse of lime sludge from immediate one-step lime precipitation process as a coagulant (aid) in slaughterhouse wastewater treatment. J. Environ. Manag. 342, 118278 https://doi.org/10.1016/j.jenvman.2023.118278.
Mageshkumar, M., Karthikeyan, R., 2015. Modelling the kinetics of coagulation process for tannery industry effluent treatment using Moringa oleifera seeds protein. Desalin. Water Treat. 57, 14954–14964. https://doi.org/10.1080/19443994.2015.1070294.
Managing Water Report under Uncertainty and Risk. (2012), The United Nations World Water Development Report 4, Volume 1.
Manna, M., Sen, S., 2022. Advanced oxidation process: a sustainable technology for treating refractory organic compounds present in industrial wastewater. Environ. Sci. Pollut. Res. 30, 25477–25505 https://10.1007/s11356-022-19435-0.
Mark, G., Korth, H.G., Schuchmann, H.P., Von Sonntag, C., 1996. The photochemistry of aqueous nitrate ion revisited. J. Photochem. Photobiol. A Chem. 101, 89–103. https://doi.org/10.1016/S1010-6030(96)04391-2.
Matsui, Y., Fukushi, K., Tambo, N., 1998. Modeling, simulation and operational parameters of dissolved air flotation. J. Water Supply Res. Technol. Aqua 47, 9–20. https://doi.org/10.2166/aqua.1998.0003.
Metcalf & Eddy. Wastewater Engineering - Treatment and Resource Recovery, McGraw-Hill Education, 2014.
Mkilima, T., 2022. Treatment of livestock slaughterhouse wastewater by the electrochemical method using stainless steel and copper electrodes. Environ. Qual. Manag. 32 (2), 367–379. https://doi.org/10.1002/tqem.21858.
Moser, P.B., Ricci, B.C., Reis, B.G., Neta, L.S.F., Cerqueira, A.C., Amaral, M.C.S., 2018. Effect of MBR-H_2O_2/UV Hybrid pre-treatment on nanofiltration performance for the treatment of petroleum refinery wastewater. Sep. Purif. Technol. 192, 176–184. https://doi.org/10.1016/j.seppur.2017.09.070.
Musa, M.A., Idrus, S., 2021. Physical and biological treatment technologies of slaughterhouse wastewater: a review. Sustainability 13, 4656. https://doi.org/10.3390/su13094656.
Nacheva, P.Mijalova, Pantoja, M.Reyes, Serrano, E.A. Lomelí, 2011. Treatment of slaughterhouse wastewater in upflow anaerobic sludge blanket reactor. Water Sci. Technol. 63 (5), 877–884. https://doi.org/10.2166/wst.2011.265.
Nelson, M.I., Sidhu, H.S., 2009. Analysis of the activated sludge model (number 1). Appl. Math. Lett. 22, 629–635. https://doi.org/10.1016/j.aml.2008.05.003.
Nelson, M.I., Sidhu, H.S., Watt, S., Hai, F.I., 2019. Performance analysis of the activated sludge model (number 1). Food Bioprod. Process. 116, 41–53. https://doi.org/10.1016/j.fbp.2019.03.014.
Nnaji, N.J.N., Ani, J.U., Aneke, L.E., Onukwuli, O.D., Okoro, U.C., Ume, J.I., 2014. Modelling the coag-flocculation kinetics of cashew nut testa tannins in an industrial effluent. J. Ind. Eng. Chem. 20, 1930–1935. https://doi.org/10.1016/j.jiec.2013.09.013.
Palaniandy, P., Adlan, H.M.N., Aziz, H.A., Murshed, M.F., Hung, Y.-T., 2017. Dissolved air flotation (DAF) for wastewater treatment, 1st Edition Waste Treat. Serv. Util. Ind. 145–182.
Pandis, P.K., Kalogirou, C., Kanellou, E., Vaitsis, C., Savvidou, M.G., Sourkouni, G., Zorpas, A.A., Argirusis, C., 2022. Key points of advanced oxidation processes (AOPs) for wastewater, organic pollutants and pharmaceutical waste treatment: a mini review. Chem. Eng. 6 https://doi.org/10.3390/chemengineering6010008.
Park, C.G., Choi, E.S., Jeon, H.W., Lee, J.H., Sung, B.W., Cho, Y.H., Ko, K.B., 2014. Effect of nitrate on the degradation of bisphenol A by UV/H_2O_2 and ozone/H_2O_2 oxidation in aqueous solution. Desalin. Water Treat. 52, 797–804. https://doi.org/10.1080/19443994.2013.827297.
Precious Sibiya, N., Rathilal, S., Kweinor Tetteh, E., 2021. Coagulation treatment of wastewater: kinetics and natural coagulant evaluation. Molecules 26, 698. https://doi.org/10.3390/molecules26030698.
Pubchem - Neododecanoic Acid Datasheet, Available at ⟨https://pubchem.ncbi.nlm.nih.gov/compound/Fatty-acids_-C9–13-neo#section=Depositor-Supplied-Synonyms⟩ (Accessed 01 March 2023).
Qamar, M.O., Farooqi, I.H., Munshi, F.M., Alsabhan, A.H., Kamal, M.A., Khan, M.A., Alwadai, A.S., 2022. Performance of full-scale slaughterhouse effluent treatment plant (SETP). J. King Saud. Univ. - Sci. 34, 101891 https://doi.org/10.1016/j.jksus.2022.101891.
Rafique, R.F., Min, Z., Son, G., Lee, S.H., 2015. Removal of cadmium ion using micellar-enhanced ultrafiltration (MEUF) and activated carbon fiber (ACF) hybrid processes: adsorption isotherm study for micelle onto ACF micelle onto ACF. Desalin. Water Treat. 57, 7780–7788. https://doi.org/10.1080/19443994.2015.1057538.
Rodríguez-Martínez, J., Rodríguez-Garza, I., Pedraza-Flores, E., Balagurusamy, N., Sosa-Santillan, G., Garza-García, Y., 2002. Kinetics of anaerobic treatment of slaughterhouse wastewater in batch and upflow anaerobic sludge blanket reactor. Bioresour. Technol. 85, 235–241. https://doi.org/10.1016/S0960-8524(02)00141-4.
Rubio-Clemente, A., Chica, E., Peñuela, G.A., 2017. Kinetic modeling of the UV/H_2O_2 process: determining the effective hydroxyl radical concentration. Phys. -Chem. Wastewater Treat. Resour. Recovery 19–37. https://doi.org/10.5772/65096.
Sinsuw, A.A.E., Chen, T.H., Dokmaingam, P., Suriandjo, H.S., Chu, C.Y., 2023. Life cycle assessment of environmental impacts for two-stage anaerobic biogas plant between commercial and pilot scales. Int J. Hydrog. Energy. https://doi.org/10.1016/j.ijhydene.2023.06.331.
Song, W., Ravindran, V., Pirbazari, M., 2008. Process optimization using a kinetic model for the ultraviolet radiation-hydrogen peroxide decomposition of natural and synthetic organic compounds in groundwater. Chem. Eng. Sci. 63, 3249–3270. https://doi.org/10.1016/j.ces.2008.03.024.
Tchobanoglous, G., 2003. The strategic importance of decentralised wastewater management in the twenty-first century. IDA Conf. Water Reuse Desalin. 25–26.
Tchobanoglous, G., Ruppe, L., Leverenz, H., Darby, J., 2004. Decentralized wastewater management: challenges and opportunities for the twenty-first century. Water Supply 4, 95–102. https://doi.org/10.2166/ws.2004.0011.
Tetteh, E.K., Rathilal, S., 2020. EvaluatIng pre- and post-coagulation configuration of dissolved air flotation using response surface methodology. Processes 8. https://doi.org/10.3390/pr8040383.
Tortora, F., Innocenzi, V., Prisciandaro, M., Vegliò, F., Mazziotti, G., 2016. Heavy metal removal from liquid wastes by using micellar-enhanced ultrafiltration. Water, Air, Soil Pollut. 227 https://doi.org/10.1007/s11270-016-2935-7.
Valta, K., Kosanovic, T., Malamis, D., Moustakas, K., Loizidou, M., 2015. Overview of water usage and wastewater management in the food and beverage industry. Desalin. Water Treat. 53, 3335–3347. https://doi.org/10.1080/19443994.2014.934100.
Wang, S., Sahoo, K., Jena, U., Dong, H., Bergman, R., Runge, T., 2021. Life-cycle assessment of treating slaughterhouse waste using anaerobic digestion systems. J. Clean. Prod. 292 https://doi.org/10.1016/j.jclepro.2021.126038.
Wols, B.A., Harmsen, D.J.H., Beerendonk, E.F., Hofman-Caris, C.H.M., 2015. Predicting pharmaceutical degradation by UV (MP)/H_2O_2 processes: a kinetic model. Chem. Eng. J. 263, 336–345. https://doi.org/10.1016/j.cej.2014.10.101.
Wu, X., Yang, Y., Wu, G., Mao, J., Zhou, T., 2016. Simulation and optimization of a coking wastewater biological treatment process by activated sludge models (ASM). J. Environ. Manag. 165, 235–242. https://doi.org/10.1016/j.jenvman.2015.09.041.

Yaakob, M.A., Mohamed, R.M.S.R., Al-Gheethi, A.A.S., Kassim, A.H.M., 2018. Characteristics of chicken slaughterhouse wastewater. Chem. Eng. Trans. 63, 637–642. https://doi.org/10.3303/CET1863107.

Yang, Y., Pignatello, J.J., Ma, J., Mitch, W.A., 2016. Effect of matrix components on UV/H_2O_2 and UV/$S_2O_8^{2-}$ advanced oxidation processes for trace organic degradation in reverse osmosis brines from municipal wastewater reuse facilities. Water Res 89, 192–200. https://doi.org/10.1016/j.watres.2015.11.049.

Yilmaz, T., Demir, E.K., Asik, G., Başaran, S.T., Çokgör, E.U., Sözen, S., Sahinkaya, E., 2023. Effect of sludge retention time on the performance and sludge filtration characteristics of an aerobic membrane bioreactor treating textile wastewater. J. Water Process Eng. 51, 103390 https://doi.org/10.1016/j.jwpe.2022.103390.